

Published in final edited form as:

J Org Chem. 2009 August 21; 74(16): 6169–6180. doi:10.1021/jo901073v.

Development of an Automated Microfluidic Reaction Platform for Multidimensional Screening: Reaction Discovery Employing Bicyclo[3.2.1]octanoid Scaffolds

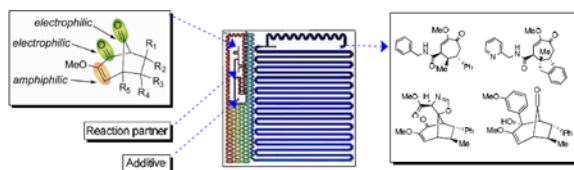
John R. Goodell[‡], Jonathan P. McMullen[†], Nikolay Zaborenko[†], Jason R. Maloney[‡], Chuan-Xing Ho[‡], Klavs F. Jensen[†], John A. Porco Jr.[‡], and Aaron B. Beeler[‡]

Aaron B. Beeler: beelera@bu.edu

[‡]Contribution from the Department of Chemistry and Center for Chemical Methodology and Library Development (CMLD-BU), Boston University, 590 Commonwealth Avenue, Boston, Massachusetts 02215

[†]Department of Chemical Engineering Massachusetts Institute of Technology 77 Massachusetts Avenue, 66-342, Cambridge, Massachusetts 02139

Abstract



An automated, silicon-based microreactor system has been developed for rapid, low-volume, multidimensional reaction screening. Use of the microfluidic platform to identify transformations of densely functionalized bicyclo[3.2.1]octanoid scaffolds will be described.

Introduction

Historically, major pharmaceutical breakthroughs have been enabled by complex chemical structures – often, complex natural products – with unique biological mechanisms.¹ Recently, there have been numerous efforts to discover new complex chemical scaffolds through organic synthesis.² As part of our interest in the synthesis of new chemotypes and structural frameworks, we recently formulated a new approach to chemical reaction discovery termed “multidimensional reaction screening.”³ In this approach, chemical reactions are evaluated using multiple variables in an array format. Efforts such as multidimensional reaction screening address an ongoing challenge in drug discovery: the decreasing availability of new chemical entities for biological screening and the need for discovery of new synthetic methodologies to access novel compounds of interest.⁴

Miniaturization and automation of biological screening have enabled an unprecedented level of throughput.⁵ However, such developments have been slower in the area of chemical reaction discovery.⁶ The recent rise of microfluidic technologies has presented an opportunity for the development of tools to enable small scale, rapid chemical reactions which may be applied to

Correspondence to: Aaron B. Beeler, beelera@bu.edu.

Supporting Information Available: Complete experimental procedures and compound characterization data including X-ray crystal structure data for **7**, **83**, **89**, **100**, and **113**. This material is available free of charge via the Internet at <http://pubs.acs.org>.

discovery endeavors.⁷ Herein, we report the development of an automated microfluidic platform and a series of multidimensional reaction screens involving bicyclo[3.2.1]octanoid scaffolds,⁸ multifunctional chemotypes⁹ presenting an array of functionality for reaction discovery (Figure 1).

Numerous reports have indicated that reactions performed within microreactors generate products in greater yield and purity and in shorter times in comparison to traditional batch conditions owing to the high heat and mass transfer and capability of obtaining wider ranges of temperature.¹⁰ The continuous flow operations and small volume inherent to microreactors enable multidimensional screening to be performed quickly while minimizing required amounts of reagents. These features also render microreactors powerful tools for screening applications involving expensive catalysts¹¹ and reagents that are difficult to synthesize in bulk.¹² Additionally, microreactors are ideal for screening highly reactive intermediates¹³ and for analyzing reaction conditions that cannot be easily achieved with conventional laboratory equipment.¹⁴

Ismagilov and coworkers recently reported studies that highlighted the advantages of microfluidic screening as an alternative to the more commonly used 96-well plates.^{15,16} In their study, reactions were preloaded into capillary cartridges as nanoliter plugs (droplets), demonstrating the potential for microfluidic reaction screening. Continuous flow screening conducted by Ley and coworkers¹⁷ represents another approach that offers many of the same advantages of microfluidics. In the current work, we expand the field of reaction screening by introducing an automated microfluidic system capable of selecting chemical reagents and solvents, as well as varying reaction times and temperature.

Results and Discussion

Automated Platform

We have constructed an automated microfluidic platform capable of conducting programmed multidimensional arrays in a sequential format (Figure 2). The ability to perform a series of specified reactions was made possible by the incorporation of a liquid handler equipped with four independently controlled sample probes. To maintain an inert environment for reagents, we designed and fabricated a 96-well reagent block that accommodates commercially available glass sleeves that are sealed with a silicon rubber septum (Figure 3). The integrity of the reagents within the block is maintained by an inert gas chamber mounted over the sample wells. This chamber also serves as a source of inert gas during reagent transfer. During the screening procedure, reagents are drawn from this reagent block by syringes and injected into the microfluidic platform as boluses.

Pulse Flow

Our specific goal was to develop a screening platform capable of executing one to several thousand analytical scale reactions. One microfluidic technique utilizes a two-phase flow system, where the reaction droplets are separated by a fluorinated carrier fluid or a gas phase.^{15,18,19} However, both of these methods have limitations in reaction screening applications. For example, solubility of the fluorinated liquid into the reaction droplet increases with higher temperatures,²⁰ and the use of a gas phase may lead to cross-contamination of the reaction droplets *via* the liquid meniscus between two droplets. Therefore, a comprehensive range of reaction conditions without cross-contamination was obtained by injecting reactions pulses into a continuous stream of solvent and by incorporating an optically triggered collection system. As illustrated in Figure 4, reagent pulses (boluses) were individually introduced into the microreactor through the liquid handler and coalesced into a single reaction pulse after entering the microreactor.²¹

A disadvantage of applying this homogenous flow style is the axial dispersion of the reaction pulses associated with laminar flow (Figure 4a).²² To account for this dispersion, an optically triggered fraction collection system was established to collect the central section of these pulses, while the tail ends were discarded (Figure 4b). The dispersion was also reduced by minimizing dead volumes and the lengths of PTFE tubing between the injector and the reactor. Furthermore, programmed delays between the reaction pulses were incorporated to prevent cross-contamination.

Reactor Design

A silicon microreactor was developed based on a design previously used for liquid-phase²³ and gas-liquid²⁴ reaction optimization. In the current design, use of T-junctions and increased serpentine channels results in improved mixing over a broader range of chemical applications compared to the previous reactor design. The microreactor layout consists of three fluid inlets, followed by an 18 μL mixing zone and a 69 μL reaction zone which terminates at the quench inlet (Figure 5). The quenched mixture flows through another mixing zone to ensure full and rapid quenching of the reaction.

The microfluidic channels and ports were etched into silicon wafers by a deep reactive ion etch (DRIE). The silicon surface was then oxidized to silica (glass) and anodically bonded to a Pyrex wafer to cap the channels, providing a glass surface that is compatible with most organic solvents. The high thermal conductivity of silicon microreactors results in fast temperature equilibration; its mechanical strength enables reactions to be investigated at pressures up to 100 bar with an appropriate packaging technique.²⁵

Fluidic connections to the chip were achieved with a compression packaging scheme (Figure 6). This compression chuck houses the microreactor and a thermoelectric (TE) element capable of heating or cooling the microreactor by adjusting the electric current.^{26,27} The wetted material of the compression piece (top half) is made from stainless steel to ensure compatibility with a broad range of reagents, while the bottom portion is constructed from aluminum to create a sufficient heat sink with high thermal conductivity for the thermoelectric device. The reaction temperature is monitored with a thermoresistor that is in direct contact with the microreactor and is inserted into the top plate.

As previously mentioned, it is necessary for each reagent pulse to enter the main reactor channels simultaneously. Accomplishing this task required the compression piece ports and the inlet channels to be designed such that the pressure drops across each reagent inlet channel were equal. Such an arrangement allows the first two reagents to enter the first T-mixer simultaneously, and the resultant stream enters the second T-mixer at the same time as the third inlet flow. This coalescence was confirmed using FEMLAB[®] simulations. At a flow rate of 15 $\mu\text{L}/\text{min}$ (5.8 min. residence time), the simulations also showed that 90 % of the mixing occurs within the first 15 % of the mixing zone (3 % of total residence time), ensuring fast mixing of the components.

Reaction times ranging from 1 to 30 minutes were controlled by adjusting the flow rate of the multi-head syringe pump. The quench stream in the reactor is an important feature that sets finite and uniform reaction times for the sequential reactions. Temperatures ranging from -30 to 100 $^{\circ}\text{C}$ were achieved by using the thermoelectric module and incorporating a sufficient heat sink. Collection of individual reaction pulses was achieved by coupling an optical trigger, an analytical scale switch, and a 96 well plate fraction collector. Analysis of the reaction screens was performed by UPLC/MS/ELSD.

Scaffold Synthesis

The synthesis of bicyclo[3.2.1]octanoid scaffolds derived from [5+2] cycloaddition of quinone monoketals and styrene derivatives was first reported by Bühi and coworkers in their work towards the synthesis of neolignan natural products.⁸ Further efforts resulted in an improved synthesis of bicyclo[3.2.1] derivatives.^{28,29} Based on these studies, we were able to develop optimized conditions for the synthesis of five bicyclo[3.2.1] substrates (Table 1) using carefully controlled addition of water. The relative stereochemistry of bicyclo[3.2.1] scaffold **7** was confirmed by X-ray crystallographic analysis.³⁰ The relative stereochemistry of bicyclo[3.2.1] substrates **8-11** was confirmed *via* ¹H coupling constant and 1D nOe analyses.³⁰

During reaction optimization, we observed that when rigorously water-free conditions were utilized for [5+2] cycloaddition of monoketal **1**³¹ and styrene (Scheme 1), the major product was diene **12** rather than the desired bicyclo[3.2.1]octanoid **7**. Ring-opened product **12** appears to arise from a retro-Dieckmann-type process with oxonium intermediate **13** and the methanol liberated during formation of oxonium intermediate **14**.³² Addition of water effectively competes with methanol to preferentially afford the desired bicyclo[3.2.1]octanoid **7**. However, the addition of more than one equivalent of water resulted in competing hydrolysis of oxonium intermediate **14** affording benzoquinone **15**. Reaction optimization revealed that the optimal amount of water needed in the reaction to maximize the yield of the desired bicyclo[3.2.1]octanoid **7** was 0.65 to 0.75 equivalents.

Multidimensional Screening of Bicyclo[3.2.1]octanoid Scaffolds

The dense functionality of multifunctional bicyclo[3.2.1]octanoid scaffolds such as **7** and **9** is highly desirable for reaction discovery. Using these scaffolds, 23 heteroatom nucleophiles, 16 carbon/dipole nucleophiles, and 16 electrophiles (reaction partners) were screened using the microfluidic platform (Figure 7). Due to the presence of multiple electrophilic centers on the substrate, reaction partners capable of tandem nucleophilic additions (e.g. **22**, **23**, **24**, **26**, and **32**) were also included. Two non-nucleophilic bases offering a range of basicity, 1,5,7-triazabicyclo[4.4.0]dec-5-ene (TBD) and 1,8-diaza-bicyclo[5.4.0]-undec-7-ene (DBU), were utilized in the multidimensional screen. A complete representation of the screening dimensions is shown in Figure 7.

Each reaction was performed using 1 μ mol (typically 0.25 mg) of substrate, with 2.0 to 3.0 equiv of reaction partner and 1.2 equiv of base with a total reaction volume of 24 μ L. The latter volume was achieved by simultaneously delivering 8 μ L of each reaction component from stock solutions in the reagent storage block (Figure 3) to the reactor. The required stock solutions were prepared in both DMSO and CH₃CN in oven-dried glass sleeves with minimal exposure to air as 0.125 M solutions of the bicyclo[3.2.1] substrates, 0.250 M solutions of the reaction partners, and 0.150 M solutions of the bases.

Reaction times of 5 min and 20 min were achieved by utilizing set flow rates of 4.5 μ L/min and 1.2 μ L/min, respectively (multi-head syringe pump with 4 - 10 mL syringes). Reactions were quenched in the reactor with 10 % v/v acetic anhydride (continuous flow) and collected into 96 well plates using UV-triggered fraction collection. The diluted reactions (final concentration = 1 mg/mL) were analyzed using UPLC/MS/ELSD³³ without further preparation. Reactions affording >20 % conversion to a major product were subsequently scaled up and isolated using traditional bench chemistry methods for further characterization of reaction products.

Analysis of UPLC/MS/ELSD data for the reaction screen indicated positive outcomes for 11 out of 23 heteroatom nucleophiles (Figure 8 and 9). All primary amine nucleophiles afforded retro-Dieckmann-type ring-opened products **72 - 93** (Tables 2 and 3). Although positive results

utilizing bicyclo[3.2.1] substrate **7** were observed when either DBU or TBD were used, higher rates of conversion were generally observed using the latter base. Interestingly, positive results utilizing substrate **9** were only observed when TBD was used as base.

During scale-up and optimization of ring-opened products such as product **72**, it became apparent that epimerization of the α -amide stereocenter was occurring, giving rise to the isolation of a mixture of diastereomers (Tables 2 and 3). It was also noted that greater rates of epimerization occurred with the stronger base, TBD, which is expected given a predicted pK_a of ~ 25 for the α -amide proton.³⁴ Thus, the observed diastereomeric ratios reported in Tables 2 and 3 are primarily dictated by deprotonation kinetics, which are in part dependent on suitable alignment of the weakly acidic proton and the amide carbonyl. The relative stereochemistry of the major diastereomer of amide **83** was confirmed by X-ray crystallographic analysis.³⁰ Conformational analysis followed by *ab initio* (B3LYP, 6-31g*) minimization of both possible diastereomers of amides **72**, **77**, and **82** (Table 2) indicated that the major diastereomers are thermodynamically favored by approximately 1-2 kcal/mol.³⁰ This data indicates that while epimerization is under kinetic control, a thermodynamic equilibrium would still exist, favoring the initially formed diastereomer (cf. **72-93**).

Heteroatom nucleophiles without an alkyl primary amine (e.g., benzylalcohol, *p*-anisidine, phenol, and *O*-benzylhydroxylamine) did not react under any of the conditions examined in the screen. This is attributed to the lower nucleophilicity of these reaction partners in comparison to those containing a primary alkyl amine. Similarly, secondary amines (e.g., *N*-methylbenzylamine, piperidine, and pyrrolidine) did not react. The only exception was the reaction between pyrrolidine (**29**) and bicyclo[3.2.1] substrate **7** which afforded tertiary amide **77**.

Reaction partners with the potential for tandem nucleophilic additions also afforded retro-Dieckmann-type ring-opened products, but did not undergo a second, intramolecular addition. As shown in Tables 2 and 3, the major isolated products were the acetylated amines and/or alcohols that were formed by quenching with acetic anhydride. While tandem addition products were not observed, tethered products were observed with diamino reaction partners **23** and **26**.³⁰ Increasing the amount of diamine to 12 equivalents effectively prevented the formation of the tethered products. The utilization of the chiral diamine, **26**, resulted in the formation of separable diastereomers (**78/79** and **89/90**). The absolute stereochemistry of **89** was confirmed by X-ray crystallographic analysis.³⁰ The relative stereochemistries of **78**, **79**, and **90** were assigned using NMR analysis.

UPLC/MS/ELSD analysis of the carbon nucleophile microfluidics screening (cf. Figure 7) also indicated positive outcomes for reactions with 3-methoxyphenylmagnesium bromide (**54**) and isonitriles **44** and **47** (Figures 8 and 9). Interestingly, structure elucidation of the reaction utilizing Grignard reagent **54** indicated that addition occurred at the enone carbonyl exclusively over the bridgehead ketone (Table 4). The addition afforded a single diastereomer, **98**, with approach occurring opposite the phenyl group.³⁵ Related additions to bicyclo[3.2.1] octanoids have been reported; however, in this case stereoselectivity was not observed.³⁶

In order to determine scope and limitation for this reaction, additional commercially available Grignard reagents were investigated using traditional bench chemistry methods. As shown in Table 4, Grignard reactions proceeded with excellent yield and afforded single diastereomers. Facial-selectivity for the addition to the diosphenol ether carbonyl was confirmed by X-ray crystallographic analysis of alcohol **100**.³⁰ As indicated in Table 4 (entry 5), only allyl magnesium bromide underwent a second addition to the bridgehead ketone to afford tertiary alcohol **102**. The relative stereochemistry of diol **102** was confirmed by 1D nOe analysis.³⁰

Furthermore, upon mild heating **102** underwent cyclization to afford polycyclic ketal **105** (Scheme 2).

Alcohol **100** derived from the addition of methyl Grignard was also treated with allyl magnesium bromide to afford diol **106**, which upon heating gave the polycyclic ketal **107**. Of the Grignard reagents investigated, only ethynyl Grignard (Table 4, entry 6) resulted in the formation of two regioisomers. In this case, addition to the enone carbonyl was still favored, but single facially-selective addition to the bridgehead ketone did occur. In order to confirm the relative stereochemistry of **104**, the tertiary alcohol was methylated using standard NaH/MeI conditions to afford the corresponding methyl ether, which was used to conduct 1D nOe analysis.^{30,37} Presumably, the smaller ethynyl functionality presents a smaller steric profile than the other Grignard reagents investigated and thus is able to approach the bridgehead ketone from the less hindered face bearing the α -methoxy enone.

Elucidation of the successful microfluidics reactions of bicyclo[3.2.1] substrates **7** and **9** with isonitriles **44** and **47** revealed that a [3+2] cycloaddition had occurred at the bridgehead ketone³⁸ in a 1:1 diastereomeric ratio affording oxazoline spirocycles (e.g., **108** and **109**; Scheme 3). Diastereoselectivity of the cycloaddition occurs through addition to the less hindered face bearing the α -methoxy enone. These structural assignments were supported by 1D nOe analyses (Scheme 2).^{30,39} The oxazoline spirocycles **108** - **111** were found to be prone to hydrolysis, affording a ring-opened formamide.^{39a} Reaction products derived from *p*-toluenesulfonyl methyl isocyanide (**44**) suffered significant decomposition while on silica and could not be cleanly isolated.

Interestingly, when an isocyanide lacking an α -acidic proton (**49**) was utilized, no reaction occurred. This suggests that the formation of an isonitrile ylide intermediate^{39a} in the presence of base is a critical step in this process. Based on this observation, we investigated an additional nitrile ylide using a standard batch reaction (Scheme 4).⁴⁰ Structure elucidation of the isolated product revealed formation of the unusual polycyclic imine **113**. The structure was confirmed by X-ray crystallographic analysis.³⁰ Selective reduction of the imine using NaBH₃CN and acetic acid afforded **114** as a single diastereomer.⁴¹

A proposed mechanism for the dipole condensation reaction is shown in Scheme 5 and takes advantage of the proximity of the diosphenol ether and bridgehead ketone on the bicyclo[3.2.1] octanoid scaffold. Addition of the dipole to the bridgehead ketone generates the nitrilium zwitterion **115**.⁴² The enol ether may then undergo intramolecular addition to the emerged nitrilium to afford oxonium intermediate **116**. Base-mediated proton transfer generates a new zwitterion **117** which undergoes intramolecular cyclization to afford **113**.

Finally, UPLC/MS/ELSD analyses of the electrophile reaction partner subset did not reveal any successful transformations. The lack of reactivity with the electrophiles was unexpected given the participation of the diosphenol ether moiety observed in the formation of polycyclic imine **113**.

Conclusion

A microfluidic reaction platform has been developed and used for multidimensional reaction screening of highly functionalized bicyclo[3.2.1]octanoid scaffolds. This study represents a successful application of microfluidics technology to reaction discovery allowing for over 1000 reactions to be screened and analyzed on an analytical scale. Use of the microfluidic platform enabled expansion of an interesting retro-Dieckmann-type fragmentation affording highly functionalized cycloheptenone derivatives. Furthermore, [3+2] cycloaddition involving the bridgehead ketone of the bicyclo[3.2.1]octanoid scaffolds and isocyanides was observed in the reaction screen. These dipole cycloadditions inspired the ultimate discovery of a stepwise

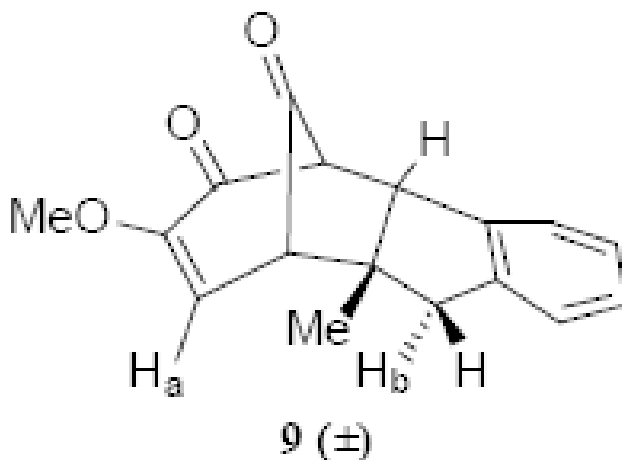
condensation of an isonitrile ylide to afford a novel polycyclic imine. Finally, use of moisture sensitive Grignard reagents with the microfluidics platform resulted in the discovery of chemo- and stereo-selective additions to the bicyclo[3.2.1]octanoid scaffolds, highlighting the overall reagent capability of the screening platform. Additional applications of microfluidics-enabled multidimensional reaction screening and expansion of the platform capabilities for reaction optimization and scaleup are currently underway and will be reported in due course.

Experimental Section

(1R,5R,6R,7R)-3-methoxy-6-methyl-7-phenylbicyclo[3.2.1]oct-3-ene-2,8-dione (\pm) (**7**)

To a oven-dried vial was added dry (1S)-(+)-10-camphorsulfonic acid (CSA) (63 mg, 0.27 mmol) followed by anhydrous CH₃CN (3 mL), water (3.7 μ L, 0.21 mmol), and β -*trans*-methylstyrene (70 μ L, 0.54 mmol). To this mixture was added 3,4,4-trimethoxycyclohexa-2,5-dienone (50 mg, 0.27 mmol) dissolved in CH₃CN (1 mL). The reaction was stirred at rt for 1.5 h, quenched with triethylamine (38 μ L) and stirred for 15 min. The solution was diluted with sat. NaHCO₃ and extracted with diethylether (x3). The organic layer was washed with brine (x1), dried over sodium sulfate, filtered, and evaporated *in vacuo*. The crude material was purified by flash chromatography (SiO₂, 20:80 EtOAc:petroleum ether) to afford **3** (43 %, 66 mg, 0.27 mmol) as clear/white crystals. m.p. = 140 - 142 °C; ¹H NMR (400 MHz, CDCl₃) δ 7.31 – 7.25 (m, 2 H), 7.24 – 7.19 (m, 1 H), 7.05 (d, *J* = 8.6 Hz, 2 H), 6.48 (d, *J* = 8.6 Hz, 1 H), 3.81 (dd, *J* = 7.0, 2.0 Hz, 1 H), 3.72 (s, 3 H), 3.20 (t, *J* = 6.5 Hz, 1 H), 3.05 (dd, *J* = 8.6, 2.1 Hz, 1 H), 2.56 (qt, *J* = 6.7 Hz, 1 H), 1.26 (d, *J* = 7.0 Hz, 3 H); ¹³C NMR (100 MHz, CDCl₃) δ 200.2, 190.3, 154.6, 138.0, 129.1, 128.6, 127.8, 118.1, 71.1, 56.0, 54.1, 49.6, 43.2, 21.7; IR (thin film) ν_{max} 2962, 1761, 1684, 1606, 1456, 1363, 1245, 1223, 1153, 1103, 1036, 753, 701 cm⁻¹; HRMS calculated for C₁₆H₁₆O₃Na: 279.0997, found: 279.1022 (M+Na).

Bicyclo[3.2.1]octanoid (\pm) **9**

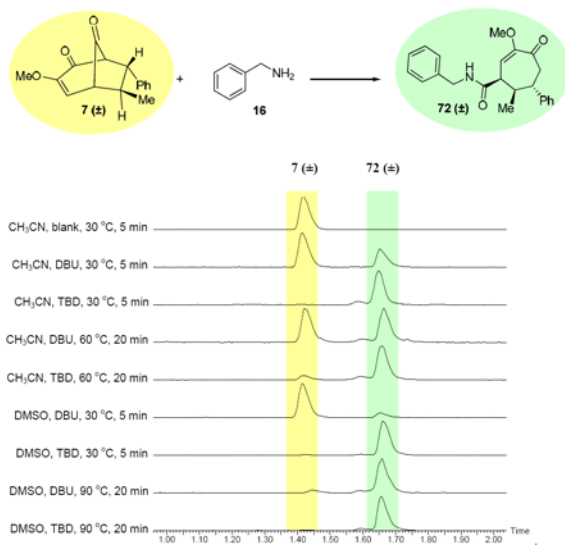


To a oven-dried vial was added dry (1S)-(+)-10-camphorsulfonic acid (CSA) (63 mg, 0.27 mmol) followed by anhydrous CH₃CN (3 mL), water (3.7 μ L, 0.21 mmol), and 2-methylindene (73 μ L, 0.54 mmol). To this mixture was added 3,4,4-trimethoxycyclohexa-2,5-dienone (50 mg, 0.27 mmol) dissolved in CH₃CN (1 mL). The reaction was stirred at rt for 1.5 h, quenched with triethylamine (38 μ L) and stirred for 15 min. The solution was diluted with sat. NaHCO₃ and extracted with diethylether (x3). The organic layer was washed with brine (x1), dried over sodium sulfate, filtered, and evaporated *in vacuo*. The crude material was purified by flash chromatography (SiO₂, 20:80 EtOAc:petroleum ether) to afford **9** (70 %, 51 mg, 0.19 mmol) as clear/white crystals; m.p. = 135 - 138 °C; ¹H NMR (400 MHz, CDCl₃) δ 7.17 – 7.10 (m, 2 H), 7.09 – 7.03 (m, 2 H), 6.04 (d, *J* = 8.3 Hz, 1 H), 4.02 (dd, *J* = 8.3, 1.8 Hz, 1 H), 3.77

(d, $J = 8.3$ Hz, 1 H), 3.35 (s, 3 H), 3.20 (d, $J = 17.3$ Hz, 1 H), 3.12 (dd, $J = 8.3, 2.0$ Hz, 1 H), 2.95 (d, $J = 17.3$ Hz, 1 H), 1.42 (s, 3 H); NOED (400 MHz, CDCl_3) irradi. δ 6.04 (H_a) 2 % enhancement at H_b , irradi. δ 3.20 (H_b) 3 % enhancement at H_a ; ^{13}C NMR (100 MHz, CDCl_3) δ 200.5, 190.3, 154.7, 143.8, 140.1, 128.0, 127.5, 126.2, 124.1, 114.2, 67.5, 58.1, 55.8, 55.1, 47.2, 42.5, 28.4; IR (thin film) ν_{max} 2962, 2923, 1762, 1685, 1608, 1458, 1218, 1141, 749 cm^{-1} ; HRMS calculated for $\text{C}_{17}\text{H}_{16}\text{O}_3\text{Na}$: 291.0997, found: 291.1026 (M+Na).

General procedure for analytical reaction screening (automated microfluidics platform)

Stock solutions of substrate (0.125 M), reaction partner (0.25 M), and base (0.15 M) were prepared in DMSO or CH_3CN (anhydrous) while maintaining dry handling. The solutions were placed in a custom designed 96-well aluminum holding block fitted with oven-dried glass sleeves. This was covered with an inert gas chamber and sealed. The block was attached to the microfluidics platform and a slow steady stream of argon was passed through the inert gas chamber. System parameters were first set to achieve 5 min reactions (microreactor residence time) at 30 °C. Longer reaction times at elevated reaction temperatures were achieved by decreasing the syringe pump flow rate and increasing the power supply to the TE heating module. Reactions were quenched on the microreactor by flowing acetic anhydride (10 % V/V in DMSO or CH_3CN) into the quench port. Individual reactions were collected into 96-well plates using optical detection. Each reaction was analyzed by UPLC/MS/ELSD (10-90 % CH_3CN , 2 min). Reactions affording >20 % conversion to a major product were subsequently scaled up and isolated, using traditional bench chemistry methods, for further characterization. A sample UPLC/ELSD Profile for substrate **7** and benzylamine (**16**) is provided below.



(1R,6S,7R,E)-N-benzyl-3-methoxy-7-methyl-4-oxo-6-phenylcyclohept-2-enecarboxamide (±) (**72**)

To an oven-dried 1 dram vial was added 3-methoxy-6-methyl-7-phenylbicyclo[3.2.1]oct-3-ene-2,8-dione (**7**) (40 mg, 0.16 mmol) and anhydrous CH_3CN (0.90 mL) followed by the addition of benzylamine (34 μL , 0.31 mmol). To this mixture was added DBU (28 μL , 0.19 mmol) in anhydrous CH_3CN (100 μL). The reaction was stirred at rt for 60 min under argon and quenched with the addition of acetic anhydride (44 μL , 0.47 mmol) in CH_3CN (400 μL). The reaction was filtered through a short plug of silica and washed with CH_3CN (2 mL \times 3, until all the product was eluted from the silica plug as indicated by TLC). The eluent was then evaporated *in vacuo*. The crude material was purified by flash chromatography (SiO_2 , 40:1 CH_2Cl_2 :MeOH) to afford **72** as a mixture of diastereomers in 20:1 ratio (dr was estimated from

crude UPLC/ELSD) (63 %, 36 mg, 0.098 mmol). Characterization data for major diastereomer: ^1H NMR (400 MHz, CDCl_3) δ 7.37 - 7.21 (m, 8 H), 7.17 - 7.12 (m, 2 H), 6.20 (d, $J = 6.1$ Hz, 1 H), 5.95 (t, $J = 5.3$ Hz, 1 H), 4.50 (dd, $J = 5.5, 4.1$ Hz, 2 H), 3.73 (s, 3 H), 3.71 (ovrlp t, $J = 5.7$ Hz, 1 H), 3.02 (dd, $J = 17.6, 11.9$ Hz, 1 H), 2.80 (dd, $J = 17.6, 1.2$ Hz, 1 H), 2.60 (dd, $J = 11.1, 9.8$ Hz, 1 H), 2.26 - 2.14 (m, 1 H), 0.88 (d, $J = 6.6$ Hz, 3 H); ^{13}C NMR (100 MHz, CDCl_3) δ 197.3, 171.2, 152.8, 143.8, 137.9, 128.8, 128.7, 128.0, 127.7, 126.9, 107.6, 55.5, 48.1, 45.9, 45.0, 44.1, 43.0, 15.3; IR (thin film) ν_{max} 3337, 2961, 2927, 1666, 1537, 1454, 1345, 1208, 1140, 701 cm^{-1} ; HRMS calculated for $\text{C}_{23}\text{H}_{26}\text{NO}_3$: 364.1913, found: 364.1937 (M+H).

(1R,6S,7R,E)-N-(4-methoxybenzyl)-3-methoxy-7-methyl-4-oxo-6-phenylcyclo hept-2-enecarboxamide (\pm) (77)

To an oven-dried 1 dram vial was added 3-methoxy-6-methyl-7-phenylbicyclo[3.2.1]oct-3-ene-2,8-dione (**7**) (40 mg, 0.16 mmol) and anhydrous CH_3CN (0.90 mL) followed by the addition of pyrrolidine (26 μL , 0.31 mmol). To this mixture was added TBD (26 mg, 0.19 mmol) in anhydrous CH_3CN (100 μL). The reaction was stirred at rt for 60 min under argon and quenched with the addition of acetic anhydride (44 μL , 0.47 mmol) in CH_3CN (400 μL). The reaction was filtered through a short plug of silica and washed with CH_3CN (2 mL \times 3, until all the product was eluted from the silica plug as indicated by TLC). The eluent was then evaporated *in vacuo*. The crude material was purified by flash chromatography (SiO_2 , 40:1 CH_2Cl_2 :MeOH) to afford **77** as a mixture of diastereomers in 9:1 ratio (dr was estimated from crude UPLC/ELSD) (56 %, 29 mg, 0.087 mmol). Characterization data for major diastereomer: ^1H NMR (400 MHz, CDCl_3) δ 7.36 - 7.22 (m, 3 H), 7.16 (d, $J = 7.4$ Hz, 2 H), 6.25 (d, $J = 5.9$ Hz, 1 H), 3.98 (t, $J = 5.5$ Hz, 1 H), 3.73 (s, 3 H), 3.67 - 3.40 (m, 4 H), 3.07 (dd, $J = 17.6, 12.5$ Hz, 1 H), 2.83 (d, $J = 17.6$ Hz, 1 H), 2.61 (dd, $J = 11.7, 9.4$ Hz, 1 H), 2.31 - 2.18 (m, 1 H), 2.06 - 1.97 (m, 2 H), 1.93 - 1.85 (m, 2 H), 0.88 (d, $J = 6.6$ Hz, 3 H); ^{13}C NMR (100 MHz, CDCl_3) δ 197.3, 170.1, 152.6, 144.2, 128.8, 127.6, 126.8, 109.2, 55.5, 48.1, 46.5, 46.0, 43.0, 40.3, 26.3, 24.1, 15.5; IR (thin film) ν_{max} 2966, 1728, 1680, 1625, 1452, 1209, 1137, 733, 703 cm^{-1} ; HRMS calculated for $\text{C}_{20}\text{H}_{25}\text{NO}_3\text{Na}$: 350.1732, found: 350.1714 (M+Na).

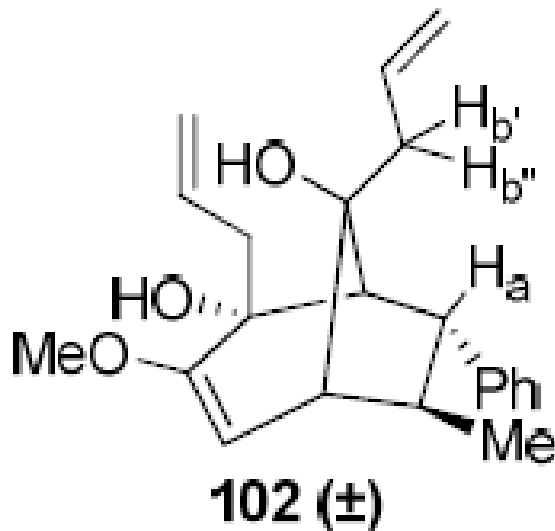
(1R,6S,7R,E)-N-(4-methoxybenzyl)-3-methoxy-7-methyl-4-oxo-6-phenylcyclohept-2-enecarboxamide (\pm) (84)

To an oven-dried 1 dram vial was added bicyclo[3.2.1]octanoid **9** (40 mg, 0.15 mmol) and anhydrous CH_3CN (0.90 mL) followed by the addition of benzylamine (30 μL , 0.30 mmol). To this mixture was added TBD (25 mg, 0.18 mmol) in anhydrous CH_3CN (100 μL). The reaction was stirred at rt for 60 min under argon and quenched with the addition of acetic anhydride (42 μL , 0.45 mmol) in CH_3CN (400 μL). The reaction was filtered through a short plug of silica and washed with CH_3CN (2 mL \times 3, until all the product was eluted from the silica plug as indicated by TLC). The eluent was then evaporated *in vacuo*. The crude material was purified by flash chromatography (SiO_2 , 40:1 CH_2Cl_2 :MeOH) to afford **84** as a mixture of diastereomers in 7:1 ratio (dr was estimated from crude UPLC/ELSD) (72 %, 40 mg, 0.11 mmol). Characterization data for major diastereomer: ^1H NMR (400 MHz, CDCl_3) δ 7.44 - 7.30 (m, 5 H), 7.20 (d, $J = 4.3$ Hz, 3 H), 7.14 (br. s., 1 H), 6.14 (d, $J = 5.9$ Hz, 1 H), 5.96 (t, $J = 5.1$ Hz, 1 H), 4.60 (dd, $J = 14.5, 5.5$ Hz, 1 H), 4.52 (dd, $J = 14.5, 5.5$ Hz, 1 H), 3.70 (s, 3 H), 3.40 (d, $J = 5.9$ Hz, 1 H), 3.06 (d, $J = 15.6$ Hz, 1 H), 2.98 (dd, $J = 11.7, 2.7$ Hz, 1 H), 2.77 - 2.68 (m, 3 H), 1.15 (s, 3 H); ^{13}C NMR (100 MHz, CDCl_3) δ 196.3, 171.3, 153.1, 143.3, 141.1, 137.9, 128.8, 128.0, 127.8, 127.4, 127.2, 124.9, 124.8, 111.9, 55.4, 51.0, 50.6, 48.7, 46.6, 44.4, 44.2, 23.4; IR (thin film) ν_{max} 3334, 2930, 1673, 1622, 1537, 1455, 1206, 1155, 1137, 1119, 754, 734, 700 cm^{-1} ; HRMS calculated for $\text{C}_{24}\text{H}_{26}\text{NO}_3$: 376.1913, found: 376.1919 (M+H).

(1R,4S,5S,6R,7R)-4-hydroxy-3-methoxy-4-(3-methoxyphenyl)-7-methyl-6-phenylbicyclo[3.2.1]oct-2-en-8-one (\pm) (98**)**

To an oven-dried vial was added 3-methoxy-6-methyl-7-phenylbicyclo[3.2.1]oct-3-ene-2,8-dione (**7**) (40 mg, 0.16 mmol) and anhydrous THF (4.0 mL). The reaction mixture was cooled to 0 °C while under argon. To this mixture was added 1.0 M 3-methoxyphenylmagnesium bromide in THF (470 μ L, 0.47 mmol) dropwise *via* syringe over 1 min while at 0 °C. The reaction was warmed to rt with continued stirring for 30 min. The reaction was cooled back down to 0 °C and quenched with the addition of water (20 μ L). This mixture was warmed to rt, diluted with water (20 mL) and extracted into CH₂Cl₂ (15 mL \times 3). The organic fractions were combined, washed with brine (20 mL), dried over sodium sulfate, filtered, and evaporated *in vacuo*. The crude product was purified by flash chromatography (SiO₂, 40:1 CH₂Cl₂:EtOAc) to afford **98** as an amorphous clear/white solid (96 %, 54 mg, 0.15 mmol). ¹H NMR (400 MHz, CDCl₃) δ 7.46 - 7.36 (m, 4 H), 7.33 - 7.27 (m, 1 H), 7.21 - 7.15 (m, 1 H), 6.83 - 6.81 (m, 1 H), 6.80 - 6.74 (m, 2 H), 5.39 (d, *J* = 7.4 Hz, 1 H), 3.74 (s, 3 H), 3.64 (s, 3 H), 3.09 (dd, *J* = 7.0, 5.9 Hz, 1 H), 2.94 (dd, *J* = 7.0, 1.6 Hz, 1 H), 2.88 - 2.78 (m, 1 H), 2.58 (dd, *J* = 7.4, 1.6 Hz, 1 H), 2.09 (s, 1 H), 1.07 (d, *J* = 7.0 Hz, 3 H); ¹³C NMR (100 MHz, CDCl₃) δ 205.7, 159.4, 155.4, 144.1, 140.6, 129.5, 128.8, 128.8, 127.2, 118.1, 113.2, 111.6, 99.5, 82.7, 63.6, 55.3, 55.1, 51.2, 50.4, 42.7, 21.5; IR (thin film) ν_{max} 3552, 2958, 1750, 1600, 1584, 1484, 1455, 1434, 1289, 1250, 1227, 1150, 1095, 1079, 1032, 784, 701 cm⁻¹; HRMS calculated for C₂₃H₂₄O₄Na: 387.1572, found: 387.1587 (M+Na).

(1R,2R,5R,6R,7R,8S)-2,8-diallyl-3-methoxy-6-methyl-7-phenylbicyclo[3.2.1] oct-3-ene-2,8-diol (\pm) (102**)**



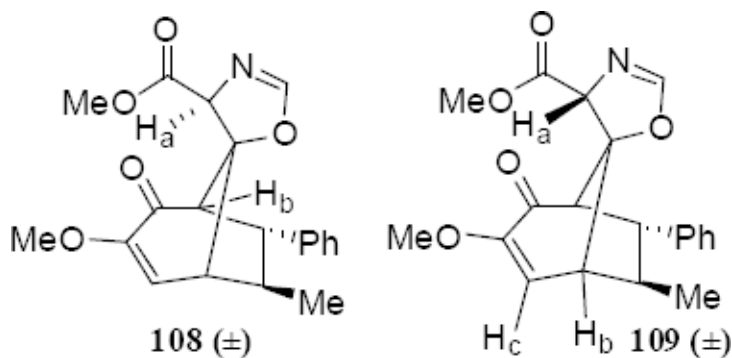
To an oven-dried vial was added 3-methoxy-6-methyl-7-phenylbicyclo[3.2.1]oct-3-ene-2,8-dione (**7**) (40 mg, 0.16 mmol) and anhydrous THF (4.0 mL). The reaction mixture was cooled to 0 °C while under argon. To this mixture was added 1.0 M allylmagnesium bromide in diethyl ether (470 μ L, 0.47 mmol) dropwise *via* syringe over 1 min while at 0 °C. The reaction was warmed to rt with continued stirring for 30 min. The reaction was cooled back down to 0 °C and quenched with the addition of water (20 μ L). This mixture was warmed to rt, diluted with water (20 mL) and extracted into CH₂Cl₂ (15 mL \times 3). The organic fractions were combined, washed with brine (20 mL), dried over sodium sulfate, filtered, and evaporated *in vacuo*. The crude product was purified by flash chromatography (SiO₂, 40:1 CH₂Cl₂:EtOAc) to afford **102** as an amorphous clear/white solid (98 %, 52 mg, 0.15 mmol). ¹H NMR (400 MHz, CDCl₃) δ 7.32 - 7.22 (m, 4 H), 7.20 - 7.13 (m, 1 H), 6.12 - 5.98 (ddt, *J* = 17.2, 10.1, 7.2 Hz, 1

H), 5.91 - 5.77 (ddt, $J = 17.4, 10.2, 7.1$ Hz, 1 H), 5.25 - 5.03 (m, 5 H), 3.56 (s, 3 H), 3.35 (dd, $J = 9.2, 5.8$ Hz, 1 H), 2.82 (dd, $J = 5.8, 2.0$ Hz, 1 H), 2.79 - 2.67 (ovrlp m, 2 H), 2.64 (d, $J = 7.4$ Hz, 2 H), 2.60 - 2.52 (m, 1 H), 2.38 (s, 1 H), 2.18 (dd, $J = 7.8, 2.0$ Hz, 1 H), 1.28 (s, 1 H), 1.18 (d, $J = 7.0$ Hz, 3 H); NOED (400 MHz, CDCl_3) irradi. δ 3.35 (H_a) 7 % enhancement at H_b , 5 % enhancement at H_b ; ^{13}C NMR (100 MHz, CDCl_3) δ 160.0, 141.5, 134.7, 134.0, 128.7, 126.1, 118.5, 118.1, 99.8, 81.5, 77.6, 55.0, 53.2, 51.4, 49.1, 43.8, 43.4, 42.6, 20.6; IR (thin film) ν_{max} 3566, 2954, 2928, 1638, 1450, 1373, 1223, 1153, 1065, 1033, 999, 912, 697 cm^{-1} ; HRMS calculated for $\text{C}_{22}\text{H}_{28}\text{O}_3\text{Na}$: 363.1936, found: 363.1942 (M+Na).

Polycyclic ketal (\pm) (105)

To a 1 dram vial was added diol **102** (20 mg, 0.059 mmol) followed by the addition of THF (1 mL). The reaction mixture was heated to 50 °C for 8 h while stirring. The reaction was concentrated and purified by flash chromatography (SiO_2 , 40:1 CH_2Cl_2 :EtOAc) to afford **105** as an amorphous clear/white solid (96 %, 19 mg, 0.056 mmol). ^1H NMR (400 MHz, CDCl_3) δ 7.31 - 7.27 (m, 4 H), 7.21 - 7.14 (m, 1 H), 6.02 - 5.89 (m, 1 H), 5.61 - 5.48 (m, 1 H), 5.20 - 5.12 (m, 2 H), 4.98 - 4.89 (m, 2 H), 3.45 (s, 3 H), 2.91 (dd, $J = 9.6, 5.7$ Hz, 1 H), 2.83 - 2.71 (m, 1 H), 2.59 (d, $J = 7.0$ Hz, 2 H), 2.48 (dd, $J = 5.7, 1.6$ Hz, 1 H), 2.32 - 2.14 (ovrlp m, 3 H), 2.07 - 1.96 (ovrlp m, 2 H), 1.24 (s, 1 H), 1.14 (d, $J = 7.0$ Hz, 3 H); ^{13}C NMR (100 MHz, CDCl_3) δ 140.0, 133.6, 133.4, 128.2, 128.1, 125.9, 119.7, 117.7, 109.7, 89.1, 81.4, 56.0, 52.5, 50.9, 49.5, 41.6, 40.6, 38.1, 36.2, 22.3; IR (thin film) ν_{max} 2953, 1498, 1456, 1447, 1311, 1217, 1154, 1134, 1096, 1064, 1032, 994, 912, 697 cm^{-1} ; HRMS calculated for $\text{C}_{22}\text{H}_{28}\text{O}_3\text{Na}$: 363.1936, found: 363.1944 (M+Na).

(1R,4'S,5R,5'R,6R,7R)-methyl 3-methoxy-7-methyl-4-oxo-6-phenyl-4'H-spiro[bicyclo[3.2.1]oct[2] ene-8,5'-oxazole]-4'-carboxylate (\pm) (108) and (1R,4'R,5R,5'R,6R,7R)-methyl 3-methoxy-7-methyl-4-oxo-6-phenyl-4'H-spiro[bicyclo[3.2.1]oct[2]ene-8,5'-oxazole]-4'-carboxylate (\pm) (109)



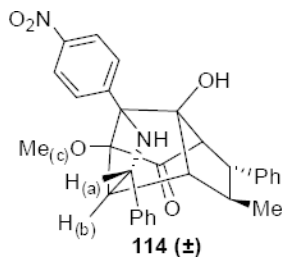
To an oven-dried 1 dram vial was added 3-methoxy-6-methyl-7-phenylbicyclo[3.2.1]oct-3-ene-2,8-dione (**7**) (40 mg, 0.16 mmol) and anhydrous CH_3CN (0.90 mL) followed by the addition of isocyanoacetate (28.3 μL , 0.312 mmol). To this mixture was added DBU (28 μL , 0.19 mmol) in anhydrous CH_3CN (100 μL). The reaction was stirred at rt for 60 min under argon, quenched by filtering through a short plug of silica and washed with CH_3CN (2 mL \times 3, until all the product was eluted from the silica plug as indicated by TLC). The eluent was then evaporated *in vacuo*. The crude material was purified by flash chromatography (SiO_2 , 1:1 EtOAc:petroleum ether) to afford **108** (35 %, 19 mg, 0.055 mmol) and **109** (37 %, 21 mg, 0.058 mmol) as amorphous clear/white solids. Characterization data for **108**: ^1H NMR (400 MHz, CDCl_3) δ 7.29 - 7.22 (m, 2 H), 7.22 - 7.14 (m, 1 H), 7.08 - 7.00 (m, 3 H), 6.26 (d, $J = 8.2$, 1 H), 4.48 (s, 1 H), 3.71 (s, 3 H), 3.62 (s, 3 H), 3.51 (t, $J = 6.4$ Hz, 1 H), 3.39 (dd, $J = 6.4, 2.0$ Hz, 1 H), 3.15 (dd, $J = 8.2, 2.0$ Hz, 1 H), 2.53 (quin, $J = 6.8$ Hz, 1 H), 1.35 (d, $J = 7.0$ Hz, 3 H); NOED (400 MHz, CDCl_3) irradi. δ 4.48 (H_a) 3 % enhancement at H_b ; irradi. δ 3.39 (H_b) 2

% enhancement at H_a; ¹³C NMR (100 MHz, CDCl₃) δ 192.0, 170.6, 156.2, 153.6, 138.0, 128.7, 128.3, 127.2, 121.2, 97.5, 70.9, 68.7, 55.4, 52.4, 51.4, 48.1, 46.6, 20.4; IR (thin film) ν_{max} 2955, 2932, 1743, 1696, 1635, 1616, 1456, 1251, 1212, 1159, 1113, 971, 736, 701 cm⁻¹; HRMS calculated for C₂₀H₂₂NO₅: 356.1498, found: 356.1513 (M+H). Characterization data for **109**: ¹H NMR (400 MHz, CDCl₃) δ 7.29 - 7.21 (m, 2 H), 7.21 - 7.14 (m, 1 H), 7.11 (s, 1 H), 7.02 (d, *J* = 7.4 Hz, 2 H), 6.28 (d, *J* = 8.6 Hz, 1 H), 4.67 (d, *J* = 1.6 Hz, 1 H), 3.72 (s, 3 H), 3.56 (s, 3H), 3.56 (ovrlp t, *J* = 6.45 Hz, 1 H), 3.35 (dd, *J* = 6.6, 2.3 Hz, 1 H), 2.81 (dd, *J* = 8.4, 2.1 Hz, 1 H), 2.56 (d, *J* = 7.0 Hz, 1 H), 1.35 (d, *J* = 7.0 Hz, 3 H); NOED (400 MHz, CDCl₃) irradiation. δ 4.67 (H_a) 3 % enhancement at H_b, 1 % enhancement at H_c; irradiation. δ 2.81 (H_b) 2 % enhancement at H_a; ¹³C NMR (100 MHz, CDCl₃) δ 191.1, 169.0, 155.8, 154.5, 137.6, 128.6, 128.4, 127.2, 118.0, 97.3, 70.6, 65.1, 55.7, 52.3, 52.2, 51.5, 46.3, 20.5; IR (thin film) ν_{max} 2955, 2932, 1745, 1692, 1632, 1615, 1244, 1207, 1176, 1162, 1138, 1103, 1009, 971, 734, 702 cm⁻¹; HRMS calculated for C₂₀H₂₂NO₅: 356.1498, found: 356.1522 (M+H).

Polycyclic imine (±) **113**

To an oven-dried 1 dram vial was added *N*-(4-nitrobenzyl)benzimidoyl chloride (**112**) (40 mg, 0.15 mmol), 3-methoxy-6-methyl-7-phenylbicyclo [3.2.1]oct-3-ene-2,8-dione (**7**) (25 mg, 0.097 mmol) and anhydrous toluene (2 mL) followed by the addition of triethylamine (30.0 μL, 0.215 mmol). The reaction was stirred at rt for 24 h while under argon. The reaction was then evaporated *in vacuo* and purified by flash chromatography (SiO₂, 40:1 CH₂Cl₂:MeOH) to afford imine **113** as a pale yellow solid (44 %, 21 mg, 0.043 mmol). m.p. = 210 - 215 °C (dec); ¹H NMR (400 MHz, CDCl₃) δ 8.23 (d, *J* = 9.0 Hz, 2 H), 7.98 (d, *J* = 7.0 Hz, 2 H), 7.85 (d, *J* = 9.0 Hz, 2 H), 7.64 - 7.48 (m, 3 H), 7.40 - 7.28 (m, 3 H), 7.22 (d, *J* = 7.4 Hz, 2 H), 3.81 (s, 1 H), 3.52 (dd, *J* = 10.6, 5.1 Hz, 1 H), 3.41 (s, 3 H), 2.70 (dd, *J* = 5.1, 2.3 Hz, 1 H), 2.42 (s, 1 H), 2.33 (ddd, *J* = 10.3, 6.9, 2.7 Hz, 1 H), 1.89 (t, *J* = 2.3 Hz, 1 H), 1.26 (d, *J* = 7.0 Hz, 3 H); ¹³C NMR (100 MHz, CDCl₃) δ 207.9, 177.0, 147.5, 142.1, 136.8, 132.2, 130.5, 129.8, 129.2, 128.4, 128.2, 127.6, 127.3, 123.4, 103.2, 90.8, 88.4, 61.4, 57.4, 56.2, 56.1, 54.1, 40.9, 20.5; IR (thin film) ν_{max} 2959, 1750, 1603, 1518, 1497, 1448, 1349, 1271, 1151, 910, 853, 732, 697 cm⁻¹; HRMS calculated for C₃₀H₂₇N₂O₅: 495.1920, found: 495.1915 (M+H).

Polycyclic amine (±) **114**



To an oven dried 1 dram vial was added polycyclic imine (**113**) (30 mg, 0.061 mmol) followed by the addition of MeOH (1 mL). Next was added NaCNBH₃ (46 mg, 0.73 mmol) and acetic acid (42 μL, 0.73 mmol). The reaction was capped and stirred at rt for 1 h. The reaction was extracted into CH₂Cl₂ (10 mL) and washed with water (10 mL × 2) then brine (10 mL). The organic portion was dried over Na₂SO₄ and evaporated *in vacuo*. The resulting residue was purified by flash chromatography (SiO₂, 20:1 CH₂Cl₂:MeOH) to afford amine **114** as a pale yellow solid (91 %, 28 mg, 0.056 mmol). m.p. = 225 - 230 °C (dec); ¹H NMR (400 MHz, CDCl₃) δ 8.17 (d, *J* = 8.6 Hz, 2 H), 7.74 (d, *J* = 9.0 Hz, 2 H), 7.56 (d, *J* = 7.4 Hz, 2 H), 7.44 (t, *J* = 7.6 Hz, 1 H), 7.37 - 7.21 (m, 5 H), 7.14 (d, *J* = 7.4 Hz, 2 H), 5.10 (d, *J* = 2.0 Hz, 1 H), 3.80 (s, 3 H), 3.23 (dd, *J* = 10.7, 5.3 Hz, 1 H), 2.81 (d, *J* = 3.1 Hz, 1 H), 2.66 (br. s., 1 H), 2.39 (dd, *J* = 5.1, 2.3 Hz, 1 H), 2.07 - 1.94 (m, 1 H), 1.89 (br. s., 1 H), 0.95 (d, *J* = 7.0 Hz, 3 H); NOED (400 MHz, CDCl₃) irradiation. δ 5.10 (H_a) 3 % enhancement at Me_c, 5 % enhancement at

H_b; irradi. δ 3.80 (Me_c) 2 % enhancement at H_a, 3 % enhancement at H_b; ¹³C NMR (100 MHz, CDCl₃) δ 210.8, 147.5, 142.1, 139.2, 137.3, 129.0, 128.6, 128.3, 128.2, 127.3, 127.1, 127.0, 123.4, 95.2, 89.3, 79.7, 63.6, 61.0, 53.7, 53.0, 52.3, 50.6, 42.8, 20.3; IR (thin film) ν_{max} 2959, 1744, 1602, 1521, 1496, 1456, 1349, 1152, 1031, 853, 754, 699 cm⁻¹; HRMS calculated for C₃₀H₂₉N₂O₅: 497.2076, found: 497.2063 (M+H).

Supplementary Material

Refer to Web version on PubMed Central for supplementary material.

Acknowledgments

This work was generously supported by Pfizer, Inc., the NIGMS CMLD Initiative (P50 GM067041), and Merck Research Laboratories. We thank Dr. Emil Lobkovsky (Cornell University) for X-ray crystal structure analyses and Professors John Snyder, James Panek, Scott Schaus, and Michael Pollastri (Boston University) for helpful discussions. We thank the NSF-REU program (CHE-0649114) for support of Chuan-Xing Ho (Summer, 2007), the Microsystem Technology Laboratories of MIT for help with microreactor fabrication, and Dr. Edward R. Murphy for assistance and advice in establishing the microfluidics screening system.

References

- (a) Balamurugan R, Dekker FJ, Waldmann H. *Mol BioSyst* 2005;1:36. [PubMed: 16880961] (b) Arve L, Voigt T, Waldmann H. *QSAR Comb Sci* 2006;25:449.
- (a) Schreiber SL. *Science* 2000;287:1964. [PubMed: 10720315] (b) Tan DS. *Nat Chem Biol* 2005;1:74. [PubMed: 16408003] (c) Shang S, Tan DS. *Curr Opin Chem Biol* 2005;9:248. [PubMed: 15939326] (d) Wipf P, Coleman CM, Janjic JM, Iyer PS, Fodor MD, Shafer YA, Stephenson CRJ, Kendall C, Day BW. *J Comb Chem* 2005;7:322. [PubMed: 15762763] (e) Wipf P, Werner S, Woo GHC, Stephenson CRJ, Walczak MAA, Coleman CM, Twining LA. *Tetrahedron* 2005;61:11488. (f) Thomas GL, Wyatt EE, Spring DR. *Curr Opin Drug Discovery Dev* 2006;9:700. (g) Spandl RJ, Bender A, Spring DR. *Org Biomol Chem* 2008;6:1149. [PubMed: 18362950]
- Beeler AB, Su S, Singleton CA, Porco JA Jr. *J Am Chem Soc* 2007;129:1413. [PubMed: 17263426]
- For discussion of reaction screening approaches, see: (a) Weber L, Illgen K, Almstetter M. *Synlett* 1999:366. (b) Kana WM, Rosenman MM, Sakurai K, Snyder TM, Liu DR. *Nature* 2004;431:545. [PubMed: 15457254] (c) Miller SJ. *Nat Biotechnol* 2004;22:1378. [PubMed: 15529161]
- Liu B, Li S, Hu J. *Am J Pharmacogenomics* 2004;4:263. [PubMed: 15287820]
- For examples of automated screening of reaction conditions, see: (a) Harre M, Neh H, Schulz C, Tilstam U, Wessa T, Weinmann H. *Org Process Res Dev* 2001;5:335. (b) von Wangelin AJ, Neumann H, Gordes D, Klaus S, Jiao H, Spannenberg A, Kruger T, Wendler C, Thurow K, Stoll N, Beller M. *Chem Eur J* 2003;9:2273. (c) Di L, McConnell OJ, Kerns EH, Sutherland AG. *J Chromatogr B* 2004;809:231. (d) Dinter C, Weinmann H, Merten C, Schutz A, Blume T, Sander M, Harre M, Neh H. *Org Process Res Dev* 2004;8:482. (e) Rudolph J, Lormann M, Bolm C, Dahmen S. *Adv Synth Catal* 2005;347:1361.
- For recent reviews on advancements in microfluidics, see: (a) Jensen KF. *Chem Eng Sci* 2001;56:293. (b) Weigl BH, Bardell RL, Cabrera CR. *Adv Drug Del Rev* 2003;55:349. (c) Pihl J, Karlsson M, Chiu DT. *Drug Discovery Today* 2005;10:1377. [PubMed: 16253876]
- Büchi G, Mak C-P. *J Am Chem Soc* 1977;99:8073.
- For examples of multifunctional scaffolds, see: (a) Couladouros EA, Strongilos AT. *Angew Chem Int Ed* 2002;41:3677. (b) Kumagai N, Muncipinto G, Schreiber SL. *Angew Chem Int Ed* 2006;45:3635. (c) Comer E, Rohan E, Deng L, Porco JA Jr. *Org Lett* 2007;9:2123. [PubMed: 17472394]
- For recent reviews on microfluidic reactions, see: (a) Fletcher PDI, Haswell SJ, Pombo-Villar E, Warrington BH, Watts P, Wong sYF, Zhang X. *Tetrahedron* 2002;58:4735. (b) Hessel V, Lowe H. *Chem Eng Technol* 2005;28:267. (c) Watts P, Haswell SJ. *Chem Soc Rev* 2005;34:235. [PubMed: 15726160] (d) Geyer K, Codee JDC, Seeberger PH. *Chem Eur J* 2006;12:8434. (e) Watts P, Wiles C. *Chem Commun* 2007:443.
- Allwardt A, Holzmüller-Lau S, Wendler C, Stoll N. *Catal Today* 2008;137:11.
- Yoshida J, Nagaki A, Yamada T. *Chem Eur J* 2008;14:7450.

13. Usutani H, Tomida Y, Nagaki A, Okamoto H, Nokami T, Yoshida J. *J Am Chem Soc* 2007;129:3046. [PubMed: 17323950]
14. De Mas N, Gunther A, Schmidt MA, Jensen KF. *Ind Chem Eng Res* 2003;42:698.
15. Chen DL, Ismagilov RF. *Curr Opin Chem Biol* 2006;10:226. [PubMed: 16677848]
16. Song H, Chen DL, Ismagilov RF. *Angew Chem Int Ed* 2006;45:7336.
17. (a) Baxendale IR, Griffiths-Jones CM, Ley SV, Tranmer GK. *Chem Eur J* 2006;12:4407. (b) Baxendale IR, Deeley J, Griffiths-Jones CM, Ley SV, Saaby S, Tranmer GK. *Chem Commun* 2006:2566. (c) Baumann M, Baxendale IR, Ley SV, Smith CD, Tranmer GK. *Org Lett* 2006;8:5231. [PubMed: 17078685]
18. Günther A, Jensen KF. *Lab Chip* 2006;6:1487. [PubMed: 17203152]
19. Hatakeyama T, Chen DL, Ismagilov RF. *J Am Chem Soc* 2006;128:2518. [PubMed: 16492019]
20. Gladysz, JA.; Curran, DP.; Horvath, ITE. *Handbook of Fluorous Chemistry*. 1. Wiley-VCH; 2004.
21. Garcia-Egido E, Spikmans V, Wong SYF, Warrington BH. *Lab Chip* 2003;3:73. [PubMed: 15100785]
22. Güther A, Khan SA, Thalmann M, Trachsel F, Jensen KF. *Lab Chip* 2004;4:278. [PubMed: 15269792]
23. Ratner DM, Murphy ER, Jhunjunwala M, Snyder DA, Jensen KF, Seeberger PH. *Chem Commun* 2005;5:578.
24. Murphy ER, Martinelli JR, Zaborenko N, Buchwald SL, Jensen KF. *Angew Chem Int Ed Engl* 2007;10:1734. [PubMed: 17397088]
25. Murphy ER, Inoue T, Sahoo HR, Zaborenko N, Jensen KF. *Lab Chip* 2007;7:1309. [PubMed: 17896015]
26. Albrecht J, Jensen KF. *Electrophoresis* 2006;27:4960. [PubMed: 17117380]
27. Park J, Park K, Shin K, Park H, Kim J, Kim R, Park S, Song Y. *Sensor Acuat B-Chem* 2006;117:516.
28. Collins JL, Grieco PA, Walker JK. *Tetrahedron Lett* 1997;38:1321.
29. For additional examples of [5+2] cycloadditions, see: (a) Engler TA, Letavic MA, Combrink KD, Takusagawa F. *J Org Chem* 1990;55:5810. (b) Harmata M, Rashatasakhon P. *Tetrahedron* 2003;59:2371.
30. See the Supporting Information for complete experimental details.
31. Clive DL, Fletcher SP, Liu D. *J Org Chem* 2004;69:3282. [PubMed: 15132533]
32. (a) Mak C-P, Bühi G. *J Org Chem* 1981;46:1. (b) Maki S, Asaba N, Koremura S, Yamamura S. *Tetrahedron Lett* 1992;33:4169.
33. Mazzeo JR, Neue UD, Kele M, Plumb RS. *Anal Chem* 2005;77:460 A.
34. University of Wisconsin: Bordwell pKa Table (Acidity in DMSO). [July 14, 2008]. <http://www.chem.wisc.edu/areas/reich/pkatable/>
35. (a) Reetz MT. *Angew Chem Int Ed Engl* 1984;23:556. (b) Ye J-L, Huang P-Q, Lu X. *J Org Chem* 2007;72:35. [PubMed: 17194079]
36. Shizuri Y, Okuno Y, Shigemori H, Yamamura S. *Tetrahedron Lett* 1987;28:6661.
37. For examples of *O*-methylation to obtain nOe correlations, see: (a) Komoda T, Sugiyama Y, Abe N, Imachi M, Hirota H, Koshino H, Hirota A. *Tetrahedron Lett* 2003;44:7417. (b) Najjar F, Baltas M, Gorrihion L, Moreno Y, Tzedakis T, Vail H, Andre-Barres C. *Eur J Org Chem* 2003:3335.
38. For examples of dipole additions to bridgehead ketone, see: (a) Van Leusen D, Van Leusen AM. *Organic Reactions* 2001;57:417. (b) Groselj U, Meden A, Stanovnik B, Svete J. *Tetrahedron Asymmetry* 2007;18:2365.
39. For examples of cycloadditions with isonitriles, see: (a) Soloshonok VA, Kacharov AD, Avilov DV, Ishikawa K, Nagashima N, Hayashi T. *J Org Chem* 1997;62:3470. (b) Terzidis M, Tsoleridis CA, Stephanidou-Stephanatou J. *Tetrahedron* 2007;63:7828.
40. Nair V, Sethumadhaven D, Nair SM, Viji S, Rath NP. *Tetrahedron* 2002;58:3003.
41. Kiss L, Mangelinckx S, Fulop F, De Kiimpe N. *Org Lett* 2007;9:4399. [PubMed: 17880100]
42. For examples of stepwise cycloaddition, see: (a) Cantillo D, Avalos D, Babiano R, Cintas P, Jimenez JL, Light ME, Palacios JC. *Org Lett* 2008;10:1079. [PubMed: 18278925] (b) Deng X, Mani NS. *Org Lett* 2008;10:1307. [PubMed: 18302402] (c) Xie J, Yoshida K, Takasu K, Takemoto Y. *Tetrahedron Lett* 2008;49:6910. (d) Shapiro ND, Toste FD. *J Am Chem Soc* 2008;130:9244. [PubMed: 18576648]

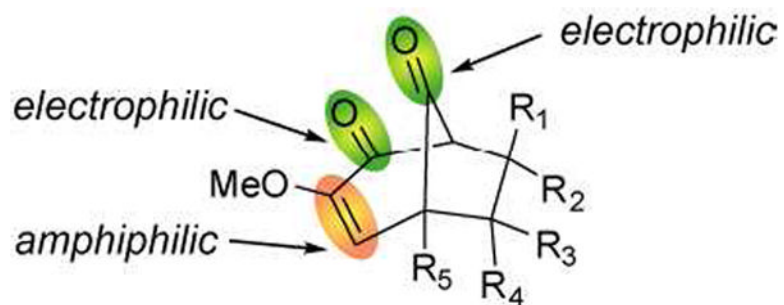


Figure 1. Diverse functionality of the bicyclo[3.2.1]octanoid scaffold for multidimensional reaction screening.

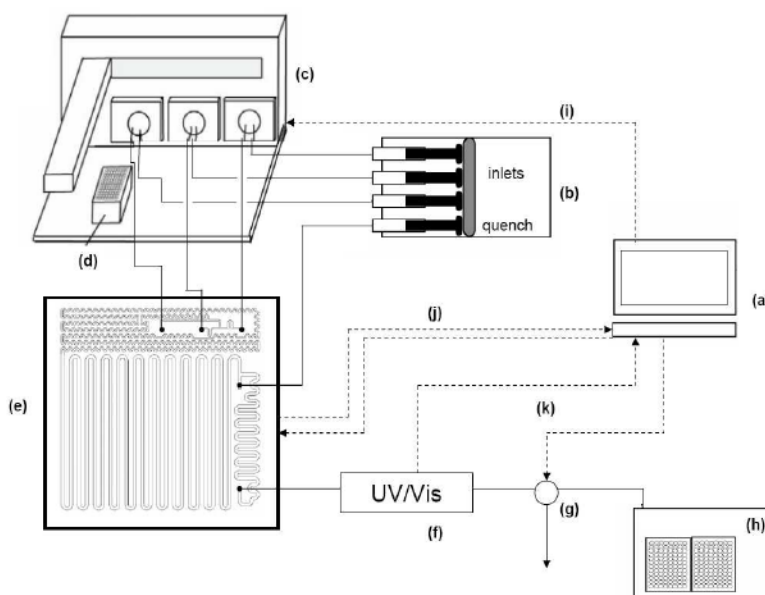


Figure 2. Automated microfluidic platform for reaction screening. Components include: (a) computer with operating software, (b) multi-head syringe pump, (c) liquid handler, (d) 96-well reagent block, (e) compression packaging that houses microreactor and thermoelectric module, (f) UV detection for optical triggering, (g) sampling valve, (h) 96-well plate fraction collector, and feedback control loops (i – k) for reagent injection, temperature control, and sample collection, respectively.

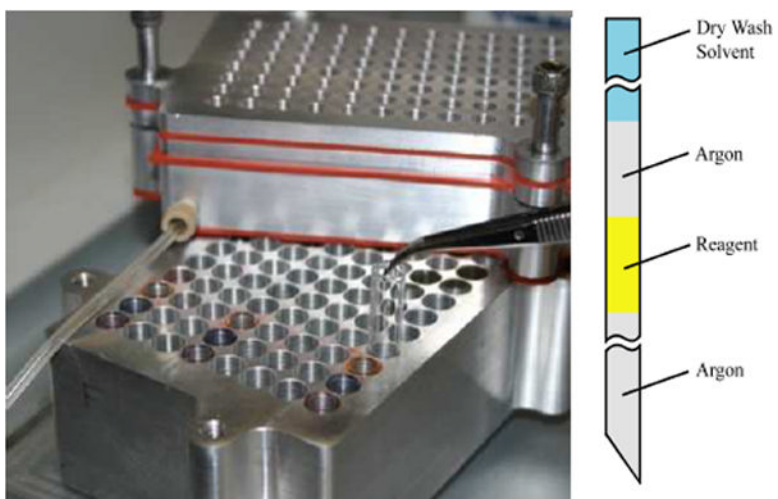


Figure 3. Reagent storage block (left) and illustration of inert handling in sample syringes (right).

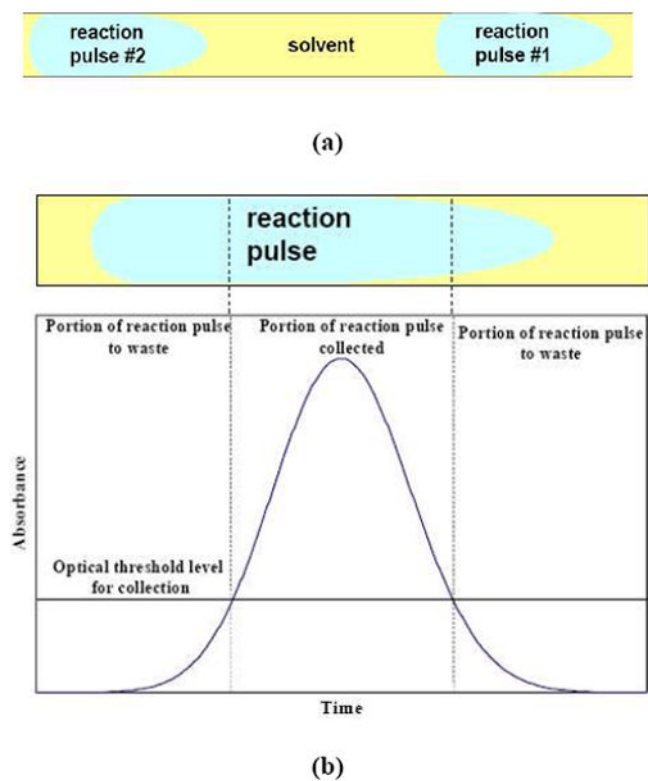


Figure 4.

a) Illustration of sequential reaction pluses and the dispersion caused by laminar flow and surface wetting. b) Example of sample collection *via* optical triggering. Collection begins and terminates once concentration of reaction pulse crosses a specified threshold, thereby enabling collection of the central portion of the pulse.

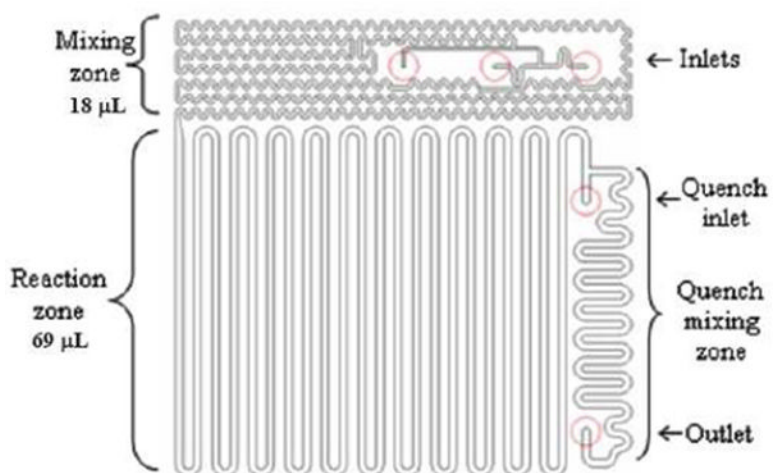


Figure 5.
Layout of the silicon microreactor used for multidimensional screens.

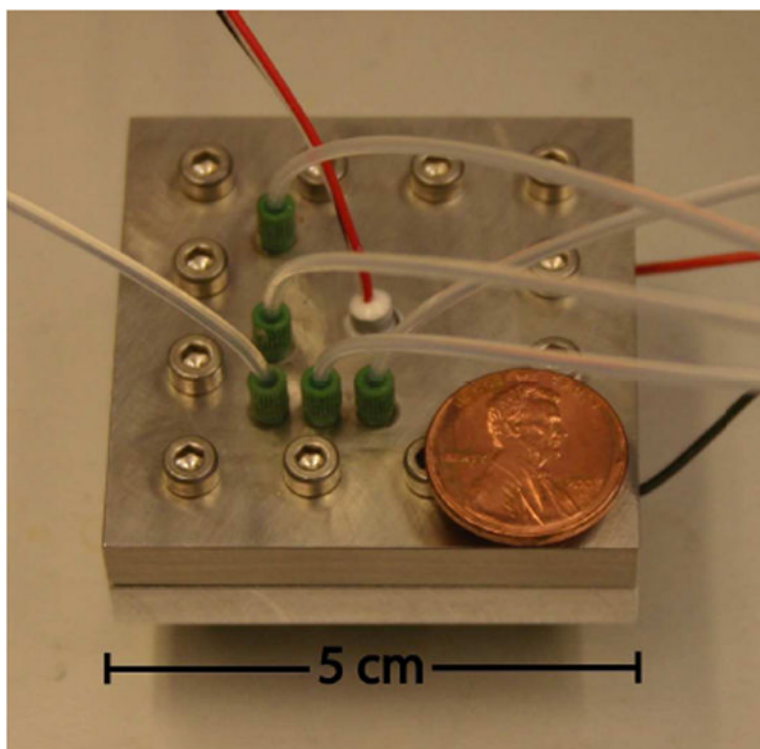


Figure 6. Compression packaging unit used in screening applications. The unit houses microreactor and thermoelectric device used for heating/cooling.

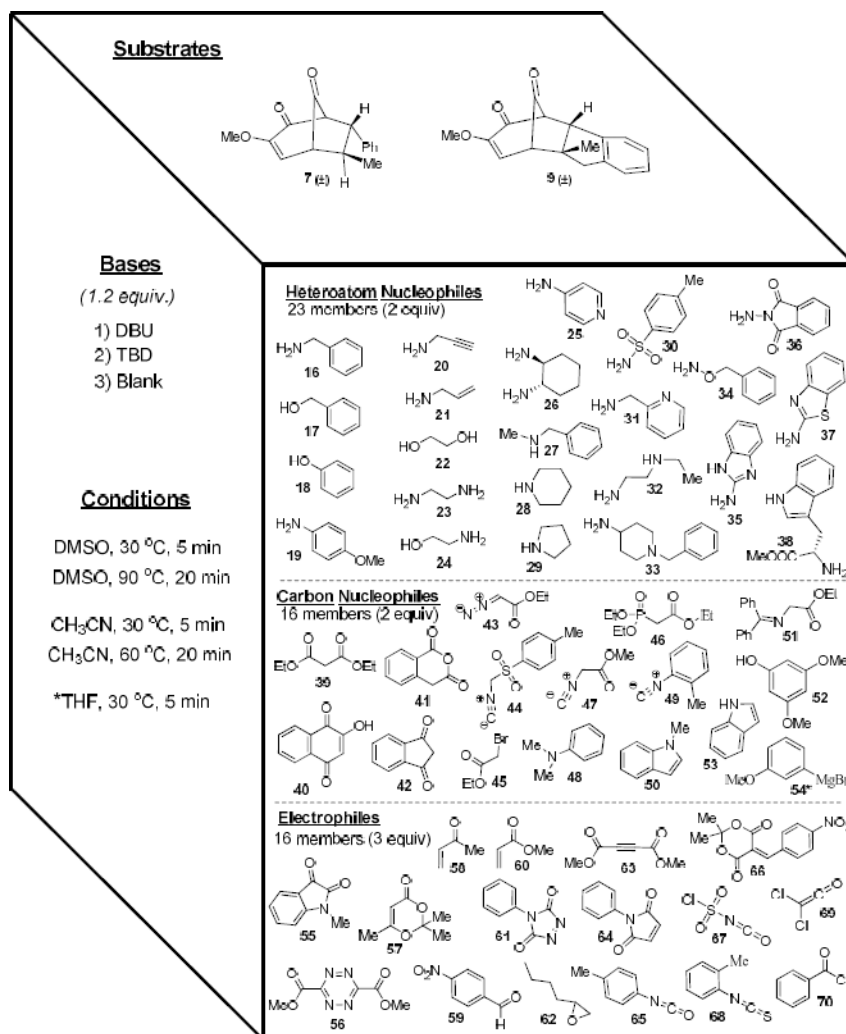


Figure 7.
Multidimensional screening parameters.

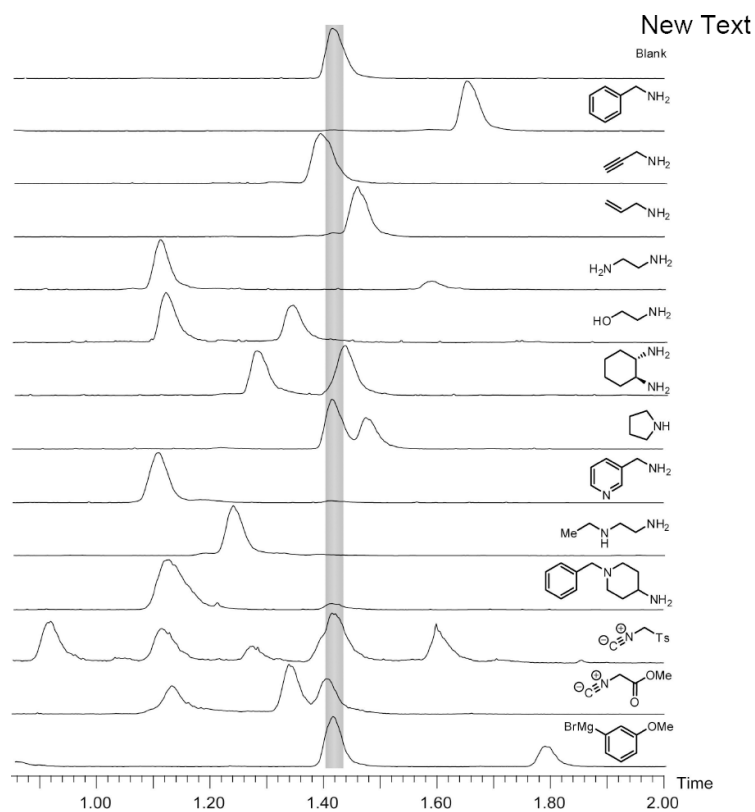


Figure 8. UPLC/ELSD results for successful transformations with bicyclo[3.2.1] substrate **7**. The shaded region represents the LC retention time for bicyclo[3.2.1] substrate **7**. Reaction conditions for displayed traces: DMSO, TBD, 5 min, 30 °C.

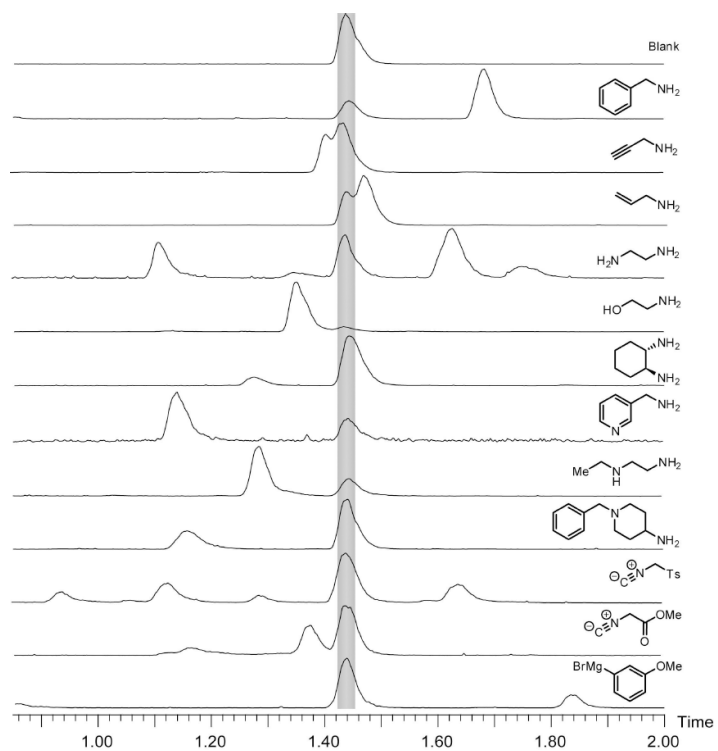
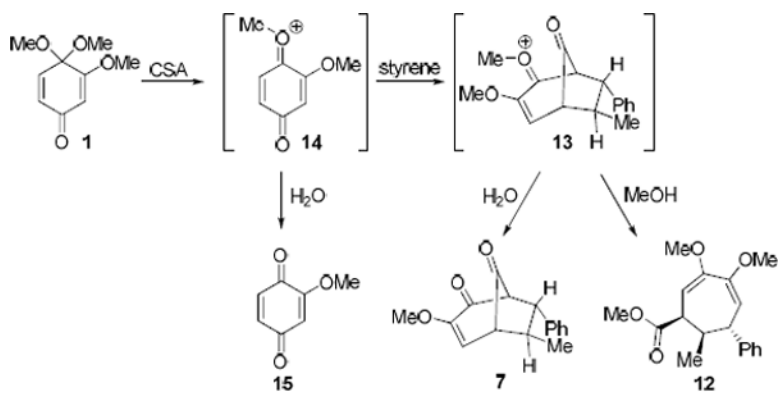
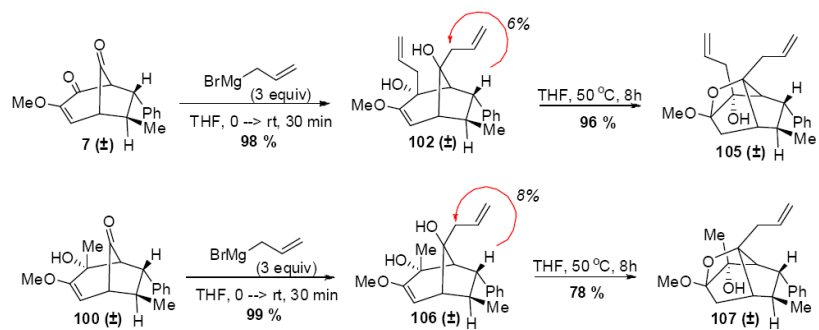


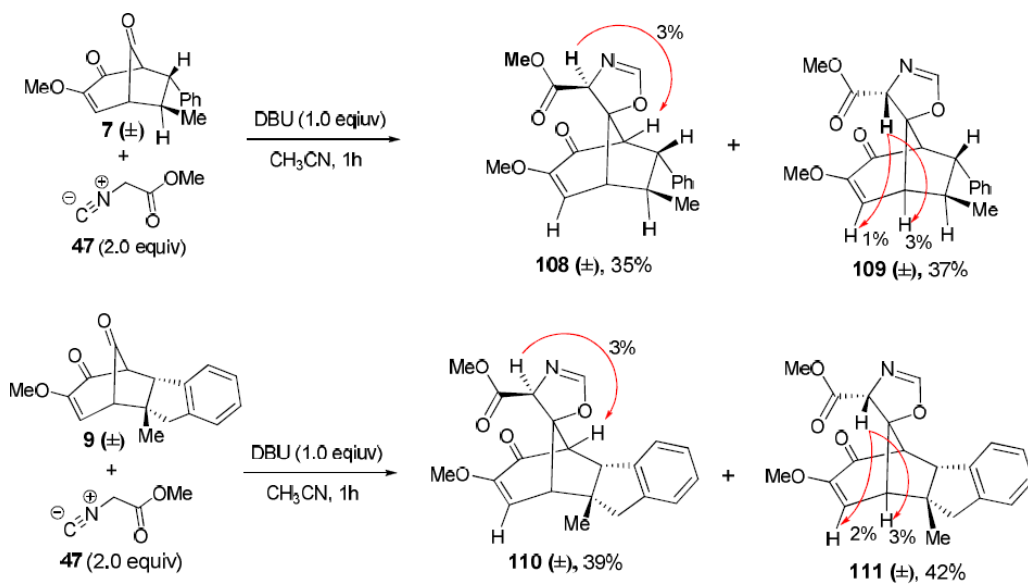
Figure 9. UPLC/ELSD results for successful transformations with bicyclo[3.2.1] substrate **9**. The shaded area represents the LC retention time for bicyclo[3.2.1] substrate **9**. Reaction conditions for displayed traces: CH_3CN , TBD, 5 min, 30 °C.



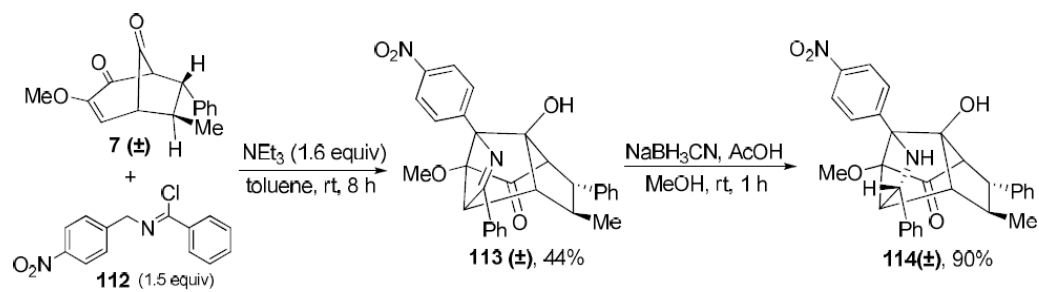
Scheme 1.
Synthesis of bicyclo[3.2.1]octanoid scaffolds.



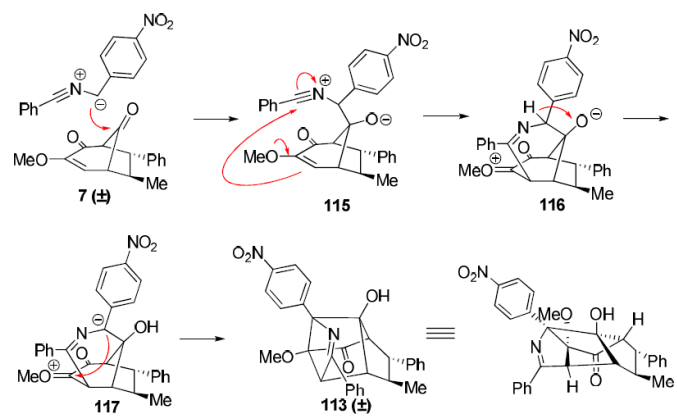
Scheme 2.
Further cyclization of allyl Grignard adducts.



Scheme 3.
Representative products for isonitrile reactions.

**Scheme 4.**

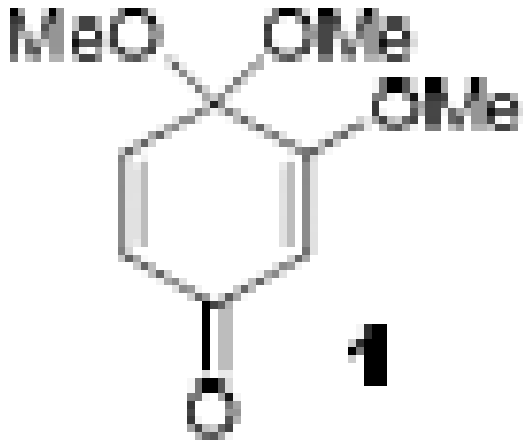
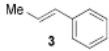
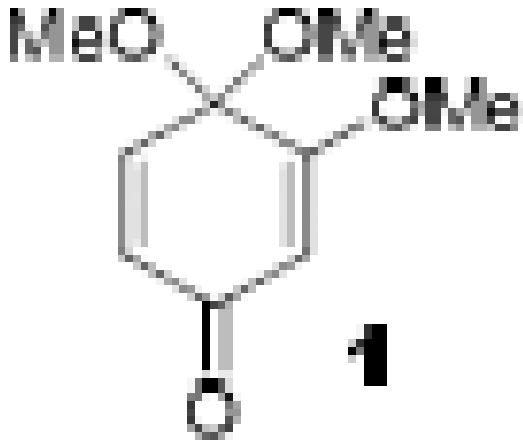
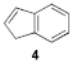
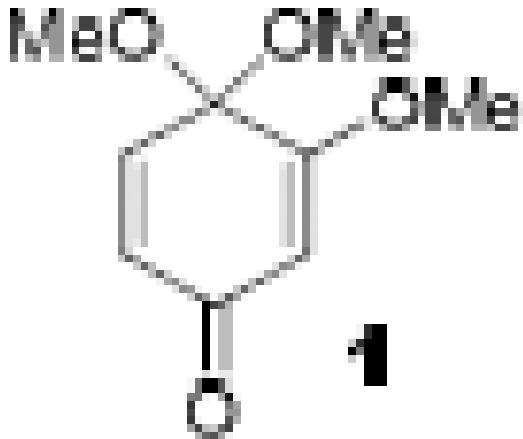
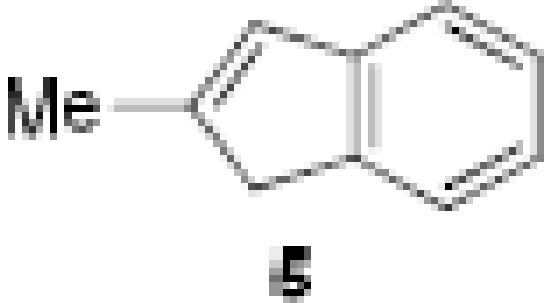
Condensation with an isonitrile ylide affords a polycyclic imine.

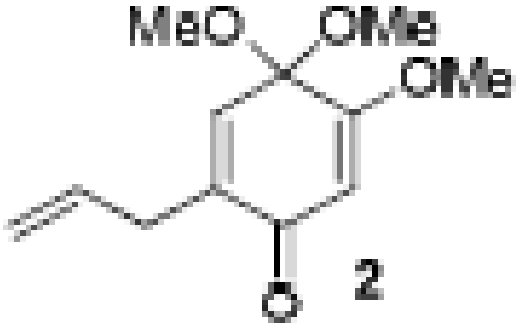
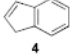
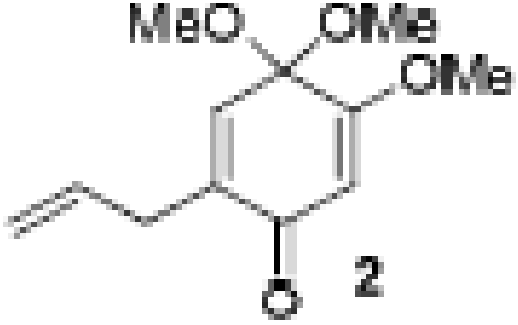
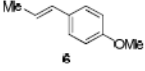


Scheme 5.
Proposed mechanism for the formation of polycyclic imine **113**.

Table 1

Synthesis of bicyclo[3.2.1]octanoid substrates ^a

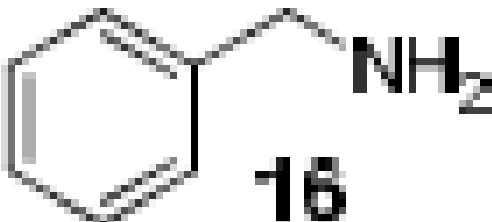
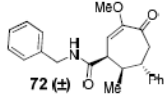
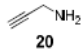
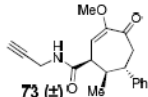

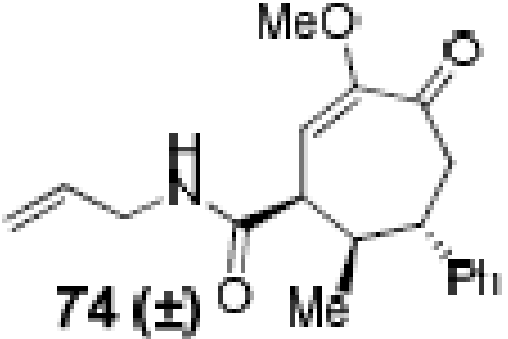
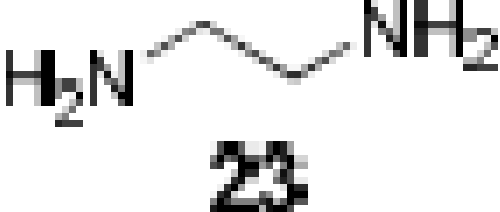
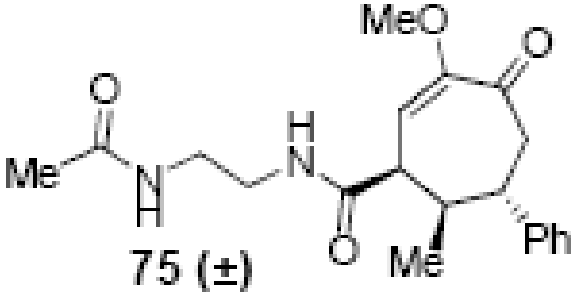
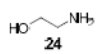
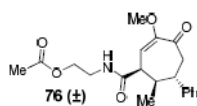
entry	monoketal	alkene
1		
2		
3		

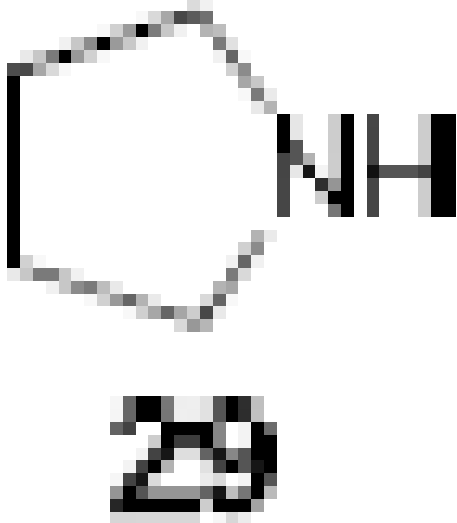
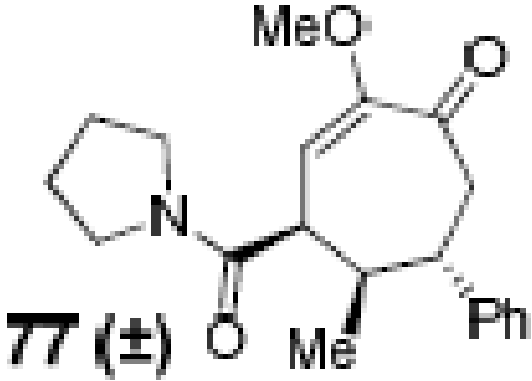
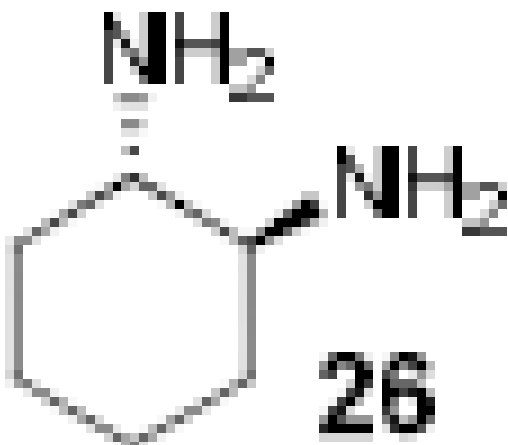
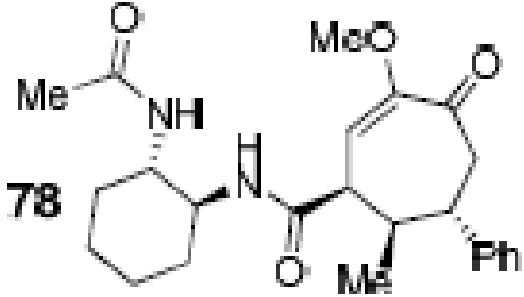
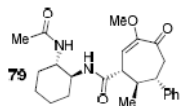
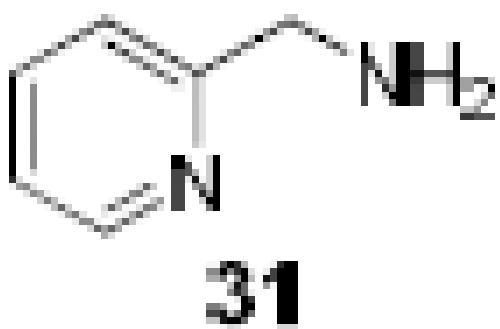
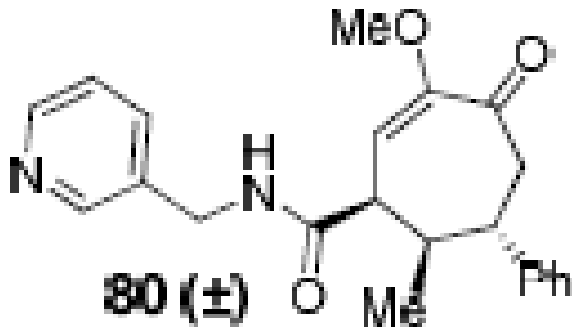
entry	monoketal	alkene
4		
5		

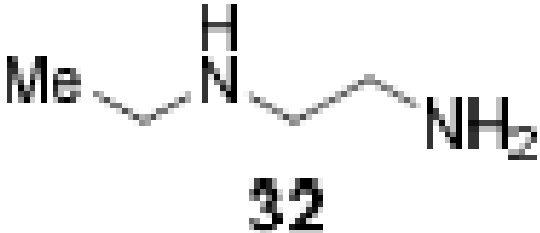
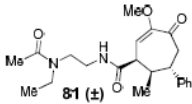
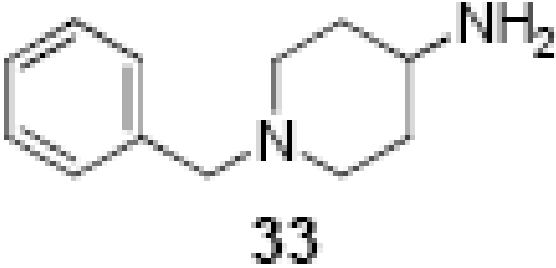
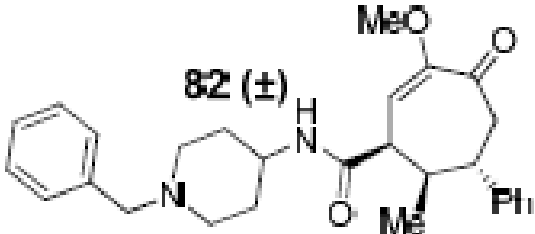
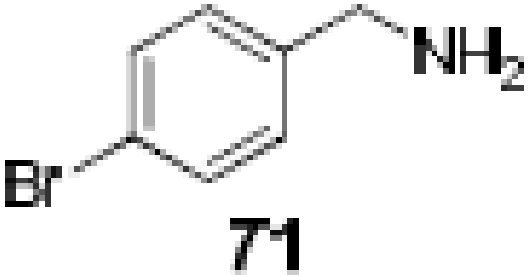
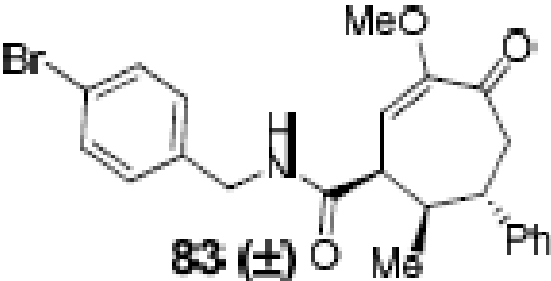
^aConditions: alkene (2.0 equiv), dry CSA (1.0 equiv), anhydrous CH₃CN, H₂O (0.75 equiv), rt, 2 h.

Table 2

Results for reactions with bicyclo[3.2.1] substrate **7**.^a

entry	nucleophile	product	yield (dr)
1	 16	 72 (±)	63 % ^b (20:1)
2	 20	 73 (±)	60 % (11:1)
3	 21	 74 (±)	54 % (13:1)
4	 23	 75 (±)	65 % ^c (14:1)
5	 24	 76 (±)	57 % (10:1)

entry	nucleophile	product	yield (dr)
6	 <p>29</p>	 <p>77 (±)</p>	56 % ^d (9:1)
7	 <p>26</p>	 <p>78</p>	35 % ^c (>25:1)
		 <p>79</p>	23 % ^c (>25:1)
8	 <p>31</p>	 <p>80 (±)</p>	55 % (>20:1)

entry	nucleophile	product	yield (dr)
9	 <p>32</p>	 <p>81 (±)</p>	40 % (10:1)
10	 <p>33</p>	 <p>82 (±)</p>	63 % (>25:1)
11	 <p>71</p>	 <p>83 (±)</p>	65 % (>25:1)

^aReaction conditions: nucleophile (2 equiv), DBU (1.2 equiv), anhydrous CH₃CN, room temp, 1 h.

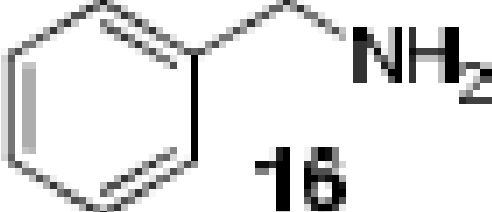
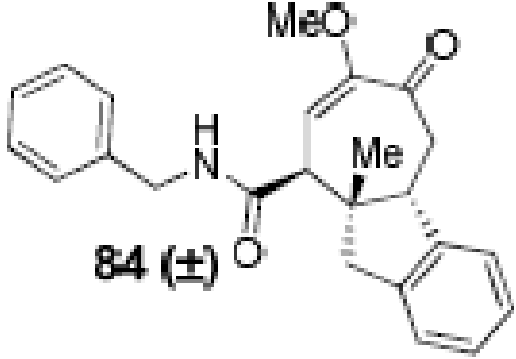
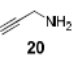
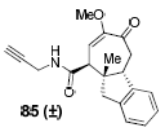

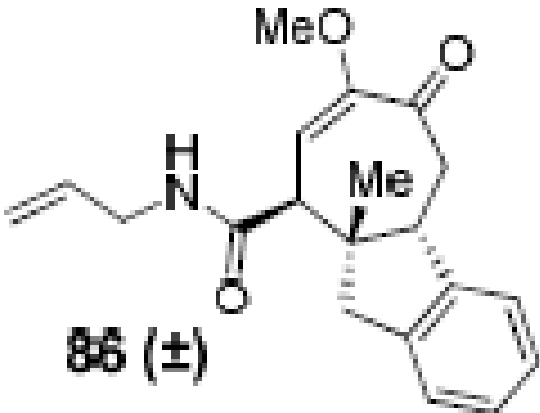

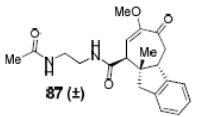
^bTBD (1.2 equiv): 50 % yield (8:1).

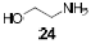
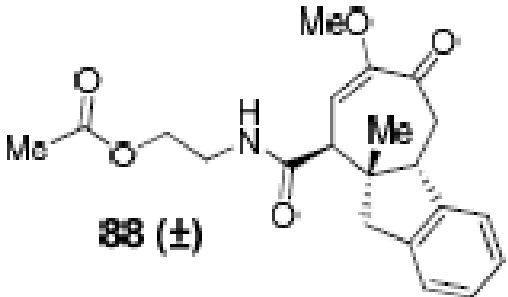
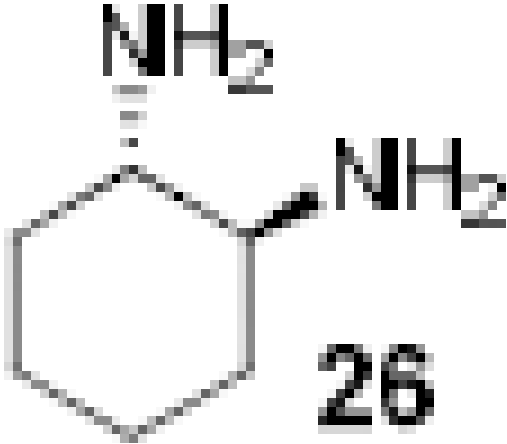
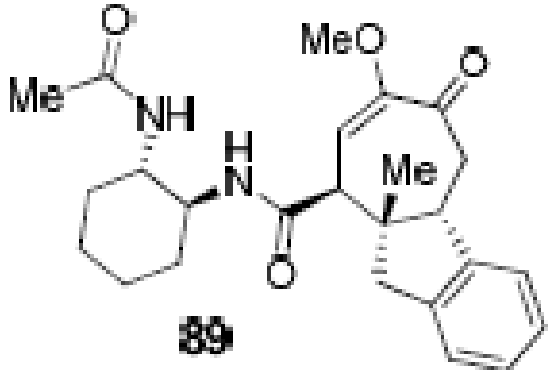
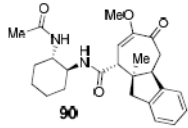
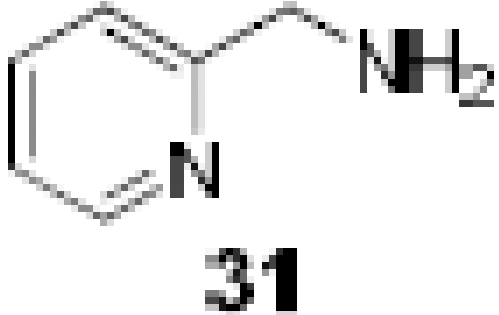
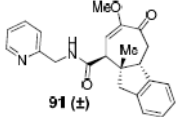
^cNucleophile (12 equiv).

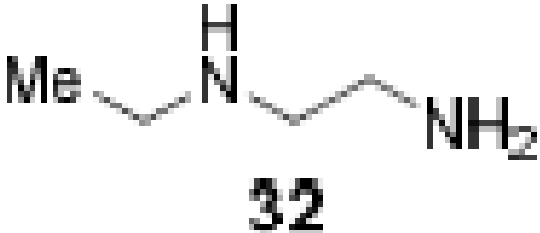
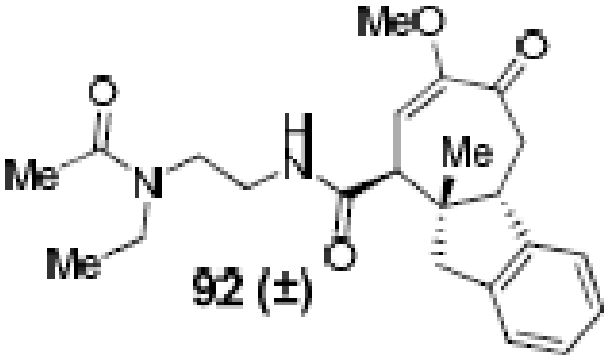
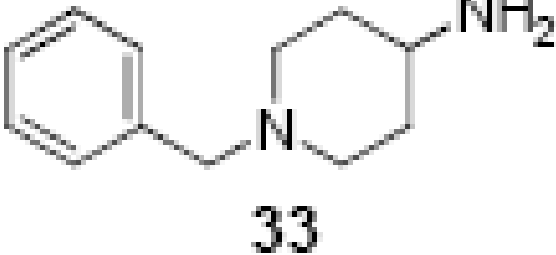
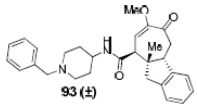
^dTBD (1.2 equiv).

Table 3

Results for reactions with bicyclo[3.2.1] substrate **9**.^a

entry	nucleophile	product	yield (dr)
1	 16	 84 (±)	72 % (7:1)
2	 20	 85 (±)	65 % (8:1)
3	 21	 86 (±)	76 % (7:1)
4	 23	 87 (±)	53 % ^b (9:1)

entry	nucleophile	product	yield (dr)
5	 24	 88 (\pm)	68 % (10:1)
6	 26	 89	27 % ^b (>25:1)
		 90	24 % ^b (>25:1)
7	 31	 91 (\pm)	64 % (8:1)

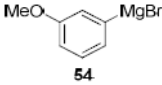
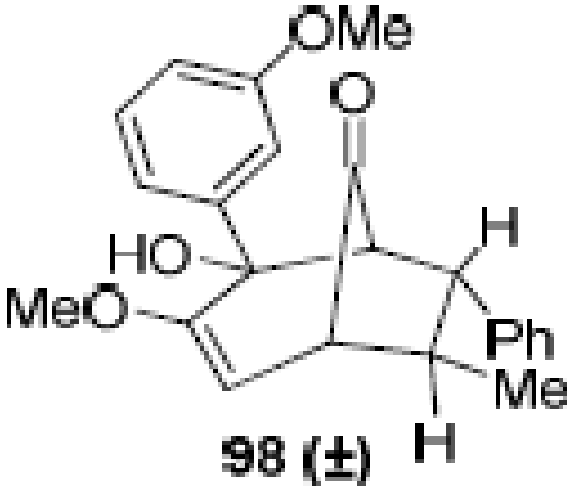
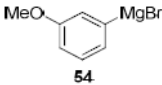
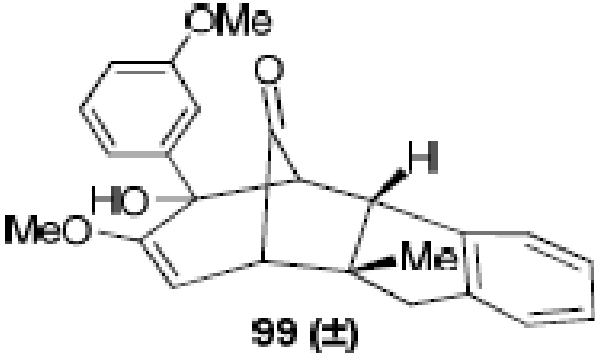

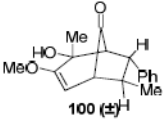
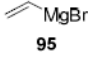
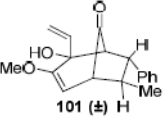
entry	nucleophile	product	yield (dr)
8	 <p>32</p>	 <p>92 (±)</p>	54 % (5:1)
9	 <p>33</p>	 <p>93 (±)</p>	49 % (>25:1)


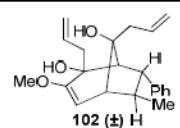
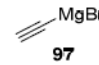
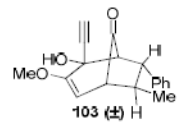
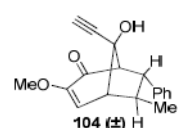
^aReaction conditions: nucleophile (2 equiv), TBD (1.2 equiv), anhydrous CH₃CN, room temp, 1 h.

^bNucleophile (12 equiv).

Table 4

Results for reactions with Grignard additions^a.

entry	sub	reagent	product	yield
1	7	 54	 98 (\pm)	96 %
2	9	 54	 99 (\pm)	99 %
3	7	 94	 100 (\pm)	95 %
4	7	 95	 101 (\pm)	91 %

entry	sub	reagent	product	yield
5	7	 96 MgBr	 102 (±) H	98 %
6	7	 97 MgBr	 103 (±) H	60 %
			 104 (±) H	30 %

^aReaction conditions: Grignard reagent (3.0 equiv), anhydrous THF, 0 ° C → rt, 30 min.